ChemMedChem

Chemistry Europe
European Chemical Societies Publishing

Accepted Article

Title: The quest for the best dual orexin receptor antagonist (daridorexant) for the treatment of insomnia disorders

Authors: Christoph Boss, John Gatfield, Christine Brotschi, Bibia Heidmann, Thierry Sifferlen, Markus von Raumer, Gunther Schmidt, Jodi T. Williams, Alexander Treiber, and Catherine Roch

To be cited as: *ChemMedChem* 10.1002/cmdc.202000453

Link to VoR: https://doi.org/10.1002/cmdc.202000453

WILEY-VCH

10.1002/cmdc.202000453

WILEY-VCH

FULL PAPER

The quest for the best dual orexin receptor antagonist (daridorexant) for the treatment of insomnia disorders

Christoph Boss*[a], John Gatfield [a], Christine Brotschi [a], Bibia Heidmann [a], Thierry Sifferlen [a], Markus von Raumer [a], Gunther Schmidt [a], Jodi T. Williams [a], Alexander Treiber [a], and Catherine Roch [a]

[a] Dr. C. Boss, Dr. J. Gatfield, Dr. C. Brotschi, Dr. B. Heidmann, Dr. T. Sifferlen, Dr. M. von Raumer, Dr. G. Schmidt, Dr. J.T. Williams, Dr. A. Treiber, Dr. C. Roch
Drug Discovery and Preclinical Research & Development
Idorsia Pharmaceuticals Ltd
Hegenheimermattweg 91; CH-4123 Allschwil / BL (Switzerland)
E-mail: christoph.boss@idorsia.com

Supporting information for this article is given via a link at the end of the document.

Abstract: Since its discovery in 1998, the orexin system is of interest to the research community as a potential therapeutic target for the treatment of sleep/wake disorders, stress and anxiety disorders, addiction or eating disorders. It consists of two G protein-coupled receptors, the orexin 1 and the orexin 2-receptor and two neuropeptides with agonistic effects, the orexin A and the orexin B-peptide. We describe our efforts leading to the identification of a promising set of dual orexin receptor antagonists (DORAs) which subsequently went through physiology-based pharmacokinetic and pharmacodynamic modelling [1] and finally led to the selection of daridorexant (**93**) currently in phase 3 clinical trials for the treatment of insomnia disorders.

Introduction

The orexin neuropeptides, orexin A (OxA) and orexin B (OxB), also known as hypocretin-1 and hypocretin-2, were discovered in 1998 by two independent research groups.[2] The two neuropeptides are secreted by a small population of excitatory neurons from the lateral hypothalamus area.[3] Orexin A and orexin B were found to bind to previously identified orphan G protein-coupled receptors (GPCR) the orexin 1 (Ox1R) and the orexin 2 receptor (Ox2R) (also termed hypocretin 1 and hypocretin 2 receptor). Both orexin neuropeptides are produced from prepro-orexin by a cascade of enzymatic reactions.[4] Orexin A, a 33 amino-acid peptide, activates both Ox1 and Ox2 receptors with similar potencies. Orexin B, which consists of 28 amino-acids, activates the Ox2R with higher potency than the Ox1R.[5] In neurons, Ox1R and Ox2R signal via various cascades to increase intracellular calcium levels pre- and/or post-synaptically, thus augmenting synaptic transmission (Figure 1).[6] The orexin system is conserved across mammalian species. OxA, containing two disulfide bridges, is conserved in rat, mouse, pig, dog and man. The linear, non-lipophilic OxB peptide from rat, mouse, pig and dog differs by maximally two amino acids (S18N) from human OxB.[7] As structural and functional homology between rat, dog and human orexin receptors and peptides are high, reliable translations of pharmacological outcomes can be made among species. While orexin-producing neurons are localized exclusively in the lateral hypothalamus, the receptors are broadly expressed all over the CNS suggesting a role in various functions. [3] Many regions express both Ox1R and Ox2R, but some express mainly one of the two, suggesting different functions of the two receptor subtypes. [8] The orexin system is indeed involved in various physiological processes. It is a key player in the control of arousal, more specifically for the maintenance of wakefulness and for sleep-to-wake transitions, taking the homeostatic, circadian and motivational necessities into account. [9] In addition, the role of the orexin system in the control of cardiovascular, behavioral, metabolic and thermoregulatory function led to the hypothesis that it integrates sleep-wake neurophysiology with energy metabolism to optimize resource utilization and energy conservation.[10] It is thus assumed, that modulation of the orexin system may have an impact on various CNS disorders such as sleep-wake disorders, addiction, eating disorders, stress and anxiety disorders. Some polymorphisms in the orexin ligand and receptor genes have been described in the human population, some of which might be linked to disease phenotypes, however with little knowledge on the mechanism of their involvement. [11] Over the last two decades, small molecule modulators of the orexin system were identified thanks to the efforts of several research teams. Antagonists of the orexin receptors, exhibiting different selectivity profiles (dual orexin receptor antagonists (DORA) or selective orexin receptor antagonists for one or the other receptor), were broadly used to investigate pharmacologically the impact of orexin receptor inhibition in physiological and pathological conditions. Orexin receptor antagonists with differential binding kinetics (surmountable versus insurmountable) properties were also identified. [12] More recently, reports on selective orexin 2 receptor agonists were published, and showed the expected wake promoting effects in healthy rodents or monkeys and wake promotion and decrease of cataplexy events in narcoleptic mice. [13]

Another important result to the field was the publication of the crystal structure of the human Ox2R, a member of the b-branch of the rhodopsin GPCR family, bound to suvorexant (**1**).[14] The authors succeeded to solve the structure at a resolution of 2.5 Angstroem, by applying lipid-mediated crystallization and protein engineering with a fusion chimera. A horseshoe resembling conformation is adopted by suvorexant (**1**) allowing optimal p-stacking and enabling binding deeply into the orthosteric receptor binding pocket. Further reports have been published describing

the crystal structure of the human Ox2R (hOx2R) and the human Ox1R (hOx1R) bound to small molecule ligands,[15] and more recently the hOx2R bound to the selective Ox2R antagonist EMPA.[16] An additional recent publication [17] discussed 14 novel structures with 10 different novel ligands in one or both the orexin receptors. This wealth of bio-structural information helps to understand the structural features resulting in selectivity for either receptor or duality of compounds and might even influence the quest for orexin receptor agonists.

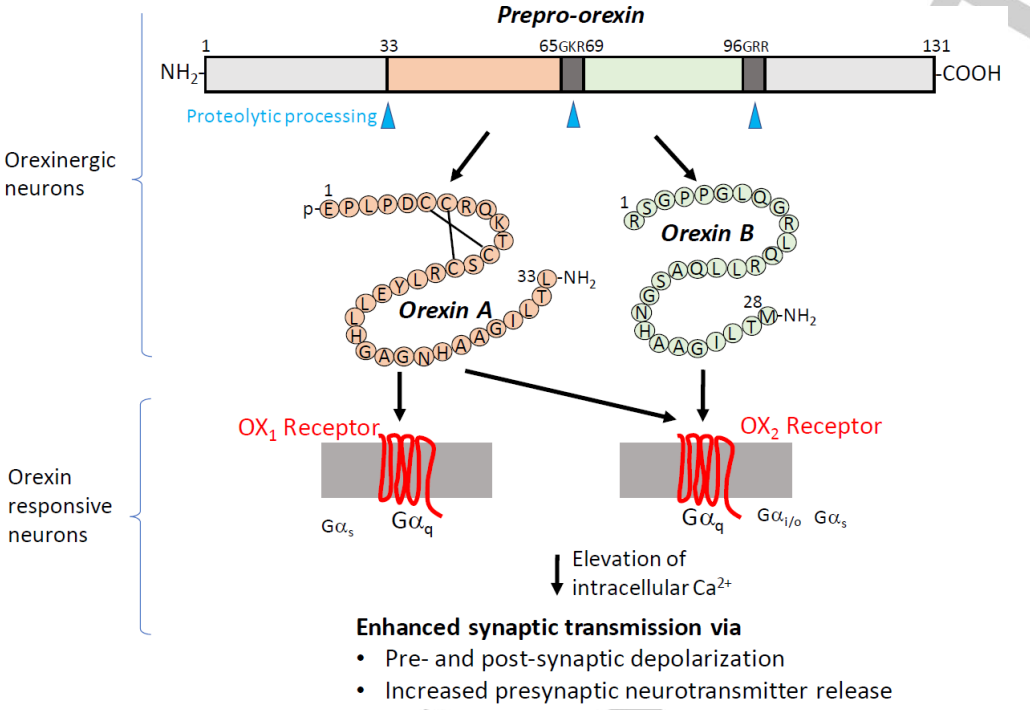

Figure 1. Orexin enhances synaptic transmission in orexin-responsive neurons of the central nervous system. A small group of orexinergic neurons in the lateral hypothalamus synthesizes prepro-orexin (131 amino acids) which is proteolytically processed by signal peptidase and pro-hormone convertases into the neuropeptides orexin A (33 amino acids, two disulfide bridges) and orexin B (28 amino acids) and stored in synaptic vesicles. Upon activation of orexinergic neurons, orexin A and orexin B are released and activate pre- and post-synaptically located OX1 and OX2 receptors that are expressed in multiple areas of the central nervous system. OX1 and OX2 receptors are G protein-coupled receptors whose activation in neurons – via various signaling cascades often involving phospholipase C (PLC) – leads to elevated intracellular calcium concentrations- and enhanced synaptic transmission.

Patients suffering from insomnia disorders are dissatisfied with their sleep quantity or quality and suffer from clinically significant negative consequences on daytime performance. It is estimated that in the US, about 50% of the adult population is dissatisfied with its sleep in at least a few nights per week. [18] Sleep problems are highly prevalent even though only about 10% of the patients fulfill the formal criteria for insomnia diagnosis. [19] Insomnia is defined by either difficulties in initiating and/or maintaining sleep or when the sleep that is obtained is non-refreshing or of poor quality. It is often associated with one or more of the following symptoms: fatigue, low energy, difficulty concentrating, mood disturbances, and decreased performance in work or at school. [20], [21] The cost for society due to lost work time, increased accident risk and higher occurrence of chronic health problems are significant. Estimates for the US published in 1994 and 2015 are above 100 billion USD per year.[22], [23] This, and the serious consequences on human health prove the high medical need for safe and effective insomnia treatments. Diagnosis of sleep disorders is often complex due to difficulties identifying the cause of the problem. This results in the fact that treatment of sleep disorders may be highly complex. One option is a nonpharmacological intervention in the form of cognitive-behavioral therapy (CBT). CBT requires increased contact with health care providers and asks for high patient compliance to result in successful outcomes. [24] The former classes of pharmacological treatments for insomnia include either targeting gamma-aminobutyric acid (GABA)-A, histamine, serotonin or melatonin receptors. The non-benzodiazepine GABA-A receptor modulators, such as zolpidem and eszopiclone are considered as standard-of-care insomnia treatments. [25] These drugs work by allosterically enhancing the effect of the most important inhibitory neurotransmitter (GABA) and result in general CNS depression to provoke sleep. [26] Such treatments are most efficient in initiating sleep. Due to their short duration of action, they are less effective in maintaining sleep. This was improved with slow-release formulations. Moreover, the approach of general CNS depression results in various safety concerns for patients. [27] Increased nighttime parasomnias (sleepwalking, eating) and increased occurrence of driving accidents due to next-day somnolence have been associated with the use of GABA modulators. [28] This resulted in modifications of labeling of GABA modulators and requests by the US Food and Drug Administration (FDA) for dose lowering for sedative hypnotic drugs in 2013. In addition, tolerance and rebound insomnia have been associated with zolpidem treatment. This led to the recommendation of intermittent use for only short periods of time for patients suffering from insomnia. [26] Novel insomnia treatment options devoid of the

drawbacks of general CNS depression would therefore represent an important step forward to treat this life-impairing condition.

Several, structurally and biochemically diverse orexin receptor antagonists have been clinically investigated over the past decade (Figure 2), resulting in a new class of pharmacological treatment with the FDA approval of suvorexant (**1**) from Merck & Co in August 2014 and of lemborexant (**2**) from Eisai in December 2019 for the treatment of insomnia. [29] The first dual orexin receptor antagonist (DORA) with clinical development history in insomnia was almorexant (**3**). [30] The compound was stopped due to tolerability issues. [31] The piperidine-based compound GSK-649868 (**4**) was studied in insomniac patients. It was put on hold due to preclinical toxicology findings although it was reported to promote sleep. The back-up compound from Merck, filorexant (**5**), also a piperidine based DORA, showed sleep promoting effects in insomniac patients in phase 2 clinical trials. [29b, 32] Finally, a selective Ox2 receptor antagonist (SO2RA), seltorexant (**6**) found in a research program at Janssen Pharmaceutica / JnJ, [33] is also studied in clinical trials by Minerva Biosciences focusing on the treatment of insomnia with or without major depressive disorder.

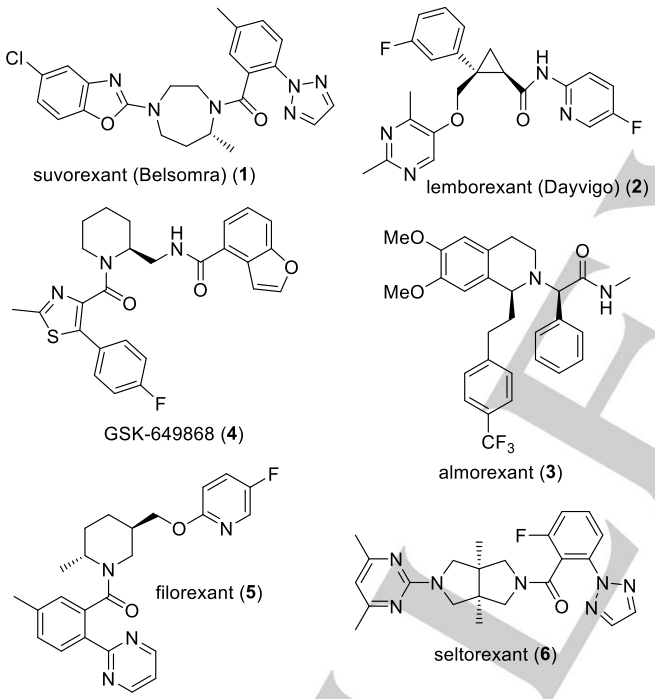

Figure 2. Structures of some orexin receptor antagonists with clinical history.

The regulation of the sleep-wake cycle is highly complex and involves different neuronal pathways. The orexin system is a key component of arousal via its excitatory projections to all the wake-promoting brain areas. Its role as a stabilizer of wakefulness, allowing long periods of wake, is well recognized. [34] Pre-clinically, DORAs have shown sleep promotion in healthy animals while maintaining sleep architecture, an advantage as compared to former sleep drugs with less selective mechanisms of action. [35] Animal model data translated into efficacy in patients suffering from insomnia. [36] However, suvorexant (**1**), the first DORA entering the market, was approved by the FDA with limitations in terms of dose due to concerns about dose-related, next-morning residual effects, as for example sedation. [37] We therefore embarked on a new program to identify potent, dual, and brain penetrant orexin antagonists starting from ACT-462206 (**7**),[38] which was in human phase I clinical trials and now is in development in veterinary medicine. We herein describe the details of our work resulting in the identification of daridorexant (ACT-541468, **93**) currently in phase 3 clinical trials for the treatment of insomnia disorders.

From a lead optimization perspective, the discovery of an insomnia drug poses specific challenges with respect to its pharmacological profile in man. Rapid sleep onset and sleep maintenance for the entire night period of about 8 hours are key attributes. Beyond target potency, brain penetration and safety aspects, particular attention was therefore drawn to the pharmacokinetic optimization in man. As outlined in our previous publication, physiology-based pharmacokinetic modelling was used to identify those compounds with the best PK-PD profile in man[1]. In practical terms, only broad acceptance criteria were defined for the progression of compounds for those assays driving human PK, i.e. metabolic stability, plasma protein binding, solubility in biological media, logD and pKa. In contrast, more stringent criteria were employed for other optimization parameters like hERG, MDR-1/P-gp efflux, or P450 inhibition.

Results and Discussion

Compound **7** (Figure 3) exhibited excellent properties as a potent, dual and brain penetrant orexin receptor antagonist. It was not a P-glycoprotein (Pgp) substrate (Efflux ratio = 1.1) based on a human multidrug resistant protein transporter assay (MDR-1), it showed human plasma protein binding (hPPB) as well as rat plasma protein binding (rPPB) of 99.3% and metabolic stability in human liver microsomes (HLM) of 140 µL min^{-1} mg^{-1}. The compound showed no significant cytochrome P450 (P450) inhibition nor time-dependent cytochrome P450 inhibition. The pharmacokinetic parameters in rats and dogs showed a short half-life ($t_{1/2}$) of 1.9 h and 1.7 h respectively. Compound **7** was

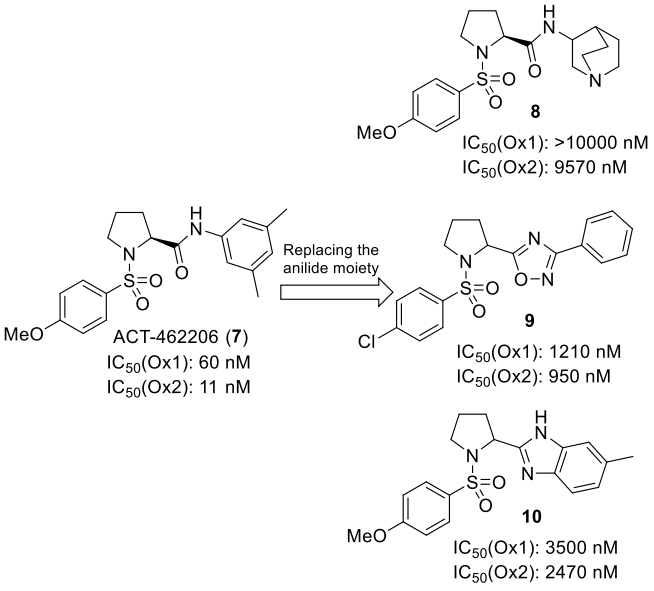

Figure 3. Where we started: ACT-462206; the quest for anilide replacements.

investigated in male Wistar rats and in male Beagle dogs implanted with radio telemetry probes recording continuously the electroencephalogram (EEG)/ the electromyogram (EMG) and locomotor activity. It dose-dependently increased both the time spent in rapid-eye-movement (REM) and non-REM (NREM) sleep. Sleep architecture was conserved, as the relative proportion of NREM and REM sleep over total sleep time were not significantly changed. [38] Compound **7** had certain limitations in its physicochemical behavior, but the overall profile made **7** an attractive starting point for further medicinal chemistry work. As depicted in Figure 3, our initial efforts targeted the replacement of the anilide moiety in **7**. Non-aromatic amides were investigated, exemplified by **8**, resulting in an almost total loss of orexin receptor antagonistic activity.

More promising results were obtained by heteroaromatic replacements of the anilide moiety by an oxadiazole unit in **9** or a benzimidazole group in **10**, resulting in activities interesting enough to continue the optimization.

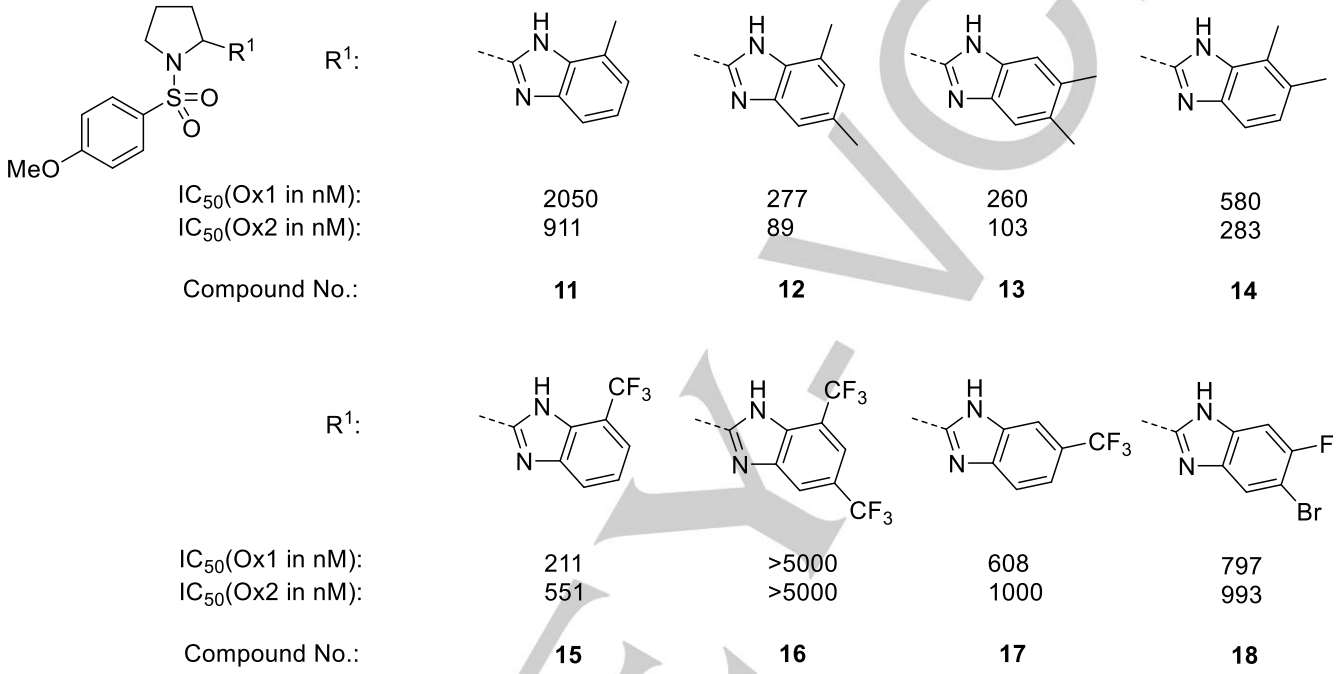

Figure 4. SAR investigation of the benzimidazole proline-sulfonamides: Substitution on the benzimidazole moiety (compounds are racemic).

In Figure 4, a summary of the first efforts on the SAR of substituents attached to the phenyl ring of the benzimidazole group is depicted. The mono-methyl-substituted compounds **10** (Figure 3) and **11** showed similar activities on the Ox1 receptor. A methyl-substituent in position 4 (**11**) resulted in improved potency on the Ox2 receptor as compared to **10**. Bis-methyl substituted benzimidazoles **12** to **14** all exhibit significantly improved antagonist activities on both, the Ox1 and Ox2 receptor. Replacing the methyl-substituent in **11** by a trifluoromethyl-substituent (**15**) resulted in a 10-fold improved Ox1 potency and only a slight improvement in Ox2 potency whereas replacement of both methyl groups from **12** with CF_3-groups in **16** resulted in a complete loss of potency. Compound **17** is the trifluoromethyl analog of **10**, exhibiting similar activity and **18** proves that halogen-substitution is tolerated. Consequently, the compounds

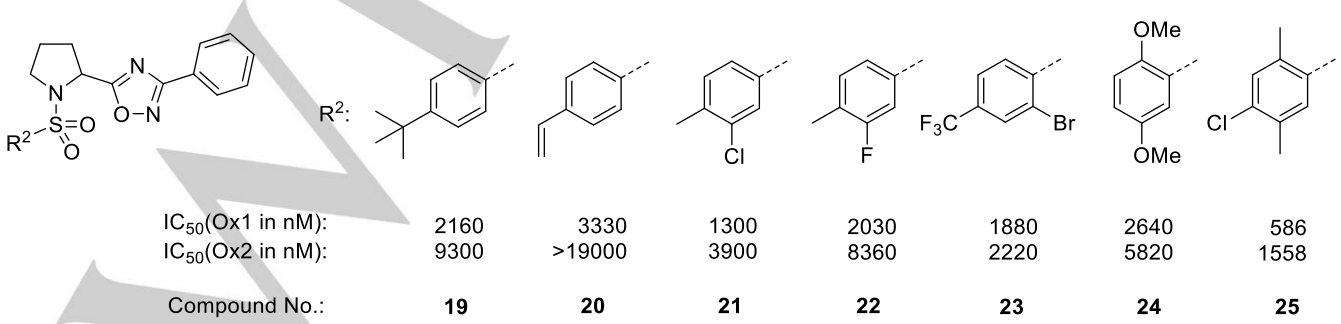

Figure 5. Sulfonamide SAR on the phenyl-oxadiazole series (compounds are racemic).

depicted in Figure 4 clearly showed that the substitution pattern on the benzimidazole moiety may significantly influence the orexin receptor antagonist potency.

We also wanted to get a first idea on the potential of the 3-phenyl substituted oxadiazole as an anilide replacement. We therefore prepared a small series of substituted phenyl-sulfonamides combined with the oxadiazole based isosteres, summarized in Figure 5 by compounds **19** to **25**. The next step was to replace the substituted phenyl sulfonamide moiety connected to the proline ring N-atom by bis-aryl-amide groups previously identified by us and others in other approaches toward orexin receptor antagonists. [4]

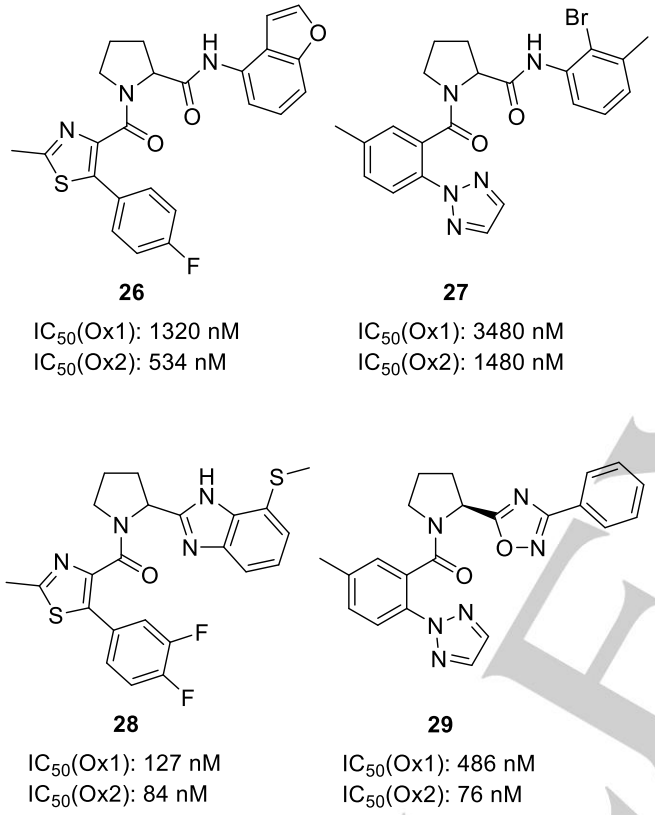

Figure 6. Switch from sulfonamide to amide.

Compounds **26** and **27** represent early examples where substituents present in **1** and **4** are differently linked to the proline template (Figure 6). The orexin receptor antagonist activities obtained were surprisingly moderate. The breakthrough came when the bis-aryl-amide moieties attached to the ring N-atom of the template were combined with the benzimidazole groups or the phenyl-oxadiazole units. The results obtained with the benzimidazole derivative **28** triggered our interest for a systematic investigation of this class of orexin antagonists. Comparison of **28** with **11**, bearing in mind the influence on orexin receptor antagonist activity of the benzimidazole substitution pattern, indicated the potential to identify promising molecules within this group of compounds. Compound **29** confirmed the potential of an aryl substituted oxadiazole moiety attached to position 2 of the template. This part of our work was described separately. [39]

A first aspect we clarified, by performing the core modification exercise summarized in Figure 7, the relevance of the proline-template.

The initial series of compounds (**30** to **34**) contained a 2-triazolo-5-methyl-benzoyl substituent attached to the ring nitrogen atom of the different scaffolds, combined with a 4-methoxy-benzimidazole moiety in α-position to the ring nitrogen atom. It showed that heterocyclic scaffolds such as thiomorpholine (**33**) or morpholine (**34**) resulted in a significant loss in orexin receptor antagonistic activity. Comparing **33** and **34** to **36** and **37** confirmed the influence of the substitution pattern at the benzimidazole moiety on activity. Moving from a pyrrolidine core (**30**) to a piperidine core (**31**) did not have a positive impact on activity either. The 2-azabicyclo [2.2.1] heptane based **32** with 1R,3S,4S-chirality, which can be looked at as 2-bridged pyrrolidines, with the bridge from C3 to C5, resulted in a very potent DORA. Further characterization of this compound was performed. Human liver microsomal (HLM) stability measurement resulted in a value of 202 µL min^{-1} mg^{-1}. The compound did not show significant P450 inhibition (3A4T IC_{50} = 18 µM (T = testosterone used as marker); 3A4M IC_{50} = 14 µM (M = midazolam used as a marker); 2C9 IC_{50} = 41 µM; 2D6 IC_{50} >50 µM) and had an acceptable IC_{50} shift in the time dependent CYP3A4 assay of 3.9-fold. In our in-house standard *in vivo* experiment where blood-brain-barrier (BBB) penetration was assessed and the compound was dosed orally at 100 mg kg^{-1} to male Wistar rats, plasma exposure measured 3h post administration was high with 6093 ng mL^{-1}. However, the corresponding brain exposure was only 682 ng g^{-1}, resulting in a B/P-ratio of 16%. Similar behavior was observed with other derivatives of this series (low B/P-ratio), indicating a possible brain penetration issue potentially due to Pgp-mediated efflux. Compound **32** was confirmed to be a Pgp substrate in the human MDR1 assay where the efflux ratio was 53 and $P_{app}AB$ was 1.1 10^{-6} $cm.s^{-1}$. Even though the orexin receptor antagonist activity was good with many derivatives (see also **35**) it was decided to abandon the template and return to the pyrrolidine core for further optimization work. Another advantage of the pyrrolidine as a template, was the commercial availability of additionally substituted derivatives. A selected overview of this work is depicted in Figure 8 with compounds **38** to **45**, and with **38** serving as the reference.

The introduction of a methylene substituent in position 4 (**39**) had no influence on orexin receptor antagonist activity. Reducing the methylene to a methyl group and having the R^1 exit vector and the substituent in a cis arrangement (**40**) was as well neutral with respect to activity. Increasing the size of the substituent in position 4 to phenyl (**42**) resulted in a slightly more dual compound, although the effect on antagonist activity was still limited. Compounds **44** and **45**, both containing a fluorine attached to position 4 but of opposite chirality, showed no positive effect of fluorine and indicated the limited influence of the chirality in this position on activity. The same observation was made when comparing **40** to **41**, even though not only the sense of chirality was different, but the substituents varied from methyl to methoxy. The introduction of an additional methyl group in position 2 (**43**), resulting in a quaternary carbon atom showed an almost 10-fold increase in Ox1R antagonist potency combined with only a 2-3-fold potency loss on the Ox2R. Furthermore, this additional methyl stabilized the chiral center and prevented racemization in the chemical transformations performed to construct the benzimidazole moiety onto the 2-methyl-proline template.

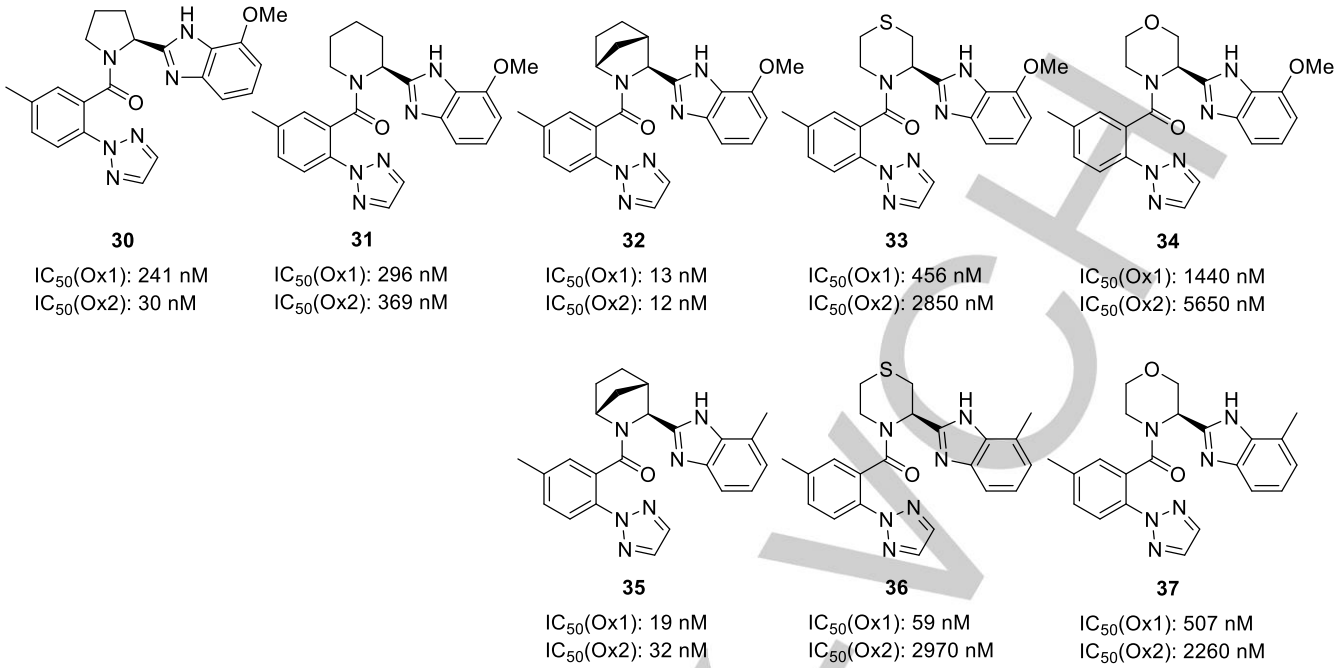

Figure 7. Core modification in the benzimidazole series of orexin receptor antagonists.

We checked for the influence of the chirality on orexin receptor antagonist potency and found the S-enantiomer as being the more potent one, in line with earlier observations. [38]
The results depicted in Table 1 gave a first insight into the effects of mono-substitution at the benzimidazole part in positions 4 and 5 (or 6 and 7; depending on the benzimidazole tautomer drawn) (Compounds **46** to **62**). The chirality of all compounds was (S) and, in order to put the results in the broadest possible perspective, the substituent connected to the proline-ring nitrogen was chosen to be the 2-triazolo-5-methyl-benzoyl moiety. For compounds **46** and **47** bearing one methyl substituent, substitution in the 4-position resulted in a significantly more active compound as compared to the 5-position. In case of the methoxy substitution, the 5-position resulted in the more active compound **49** as compared to **48**. The effect was more pronounced on the Ox2R and almost negligible on the Ox1R. A single fluorine substituent in either position (**50** vs **51**) resulted in derivatives of lower activity, whereas a single chlorine- (**52** and **53**), bromine- (**54** and **55**) or a trifluoromethyl-substituent (**56** and **57**) in either position always resulted in derivatives more active toward the Ox1R. The Ox2R/Ox1R selectivity ratio was between approximately 4-fold for **54** to 15-fold for **53** with best potencies on the Ox1R being around 11 nM.

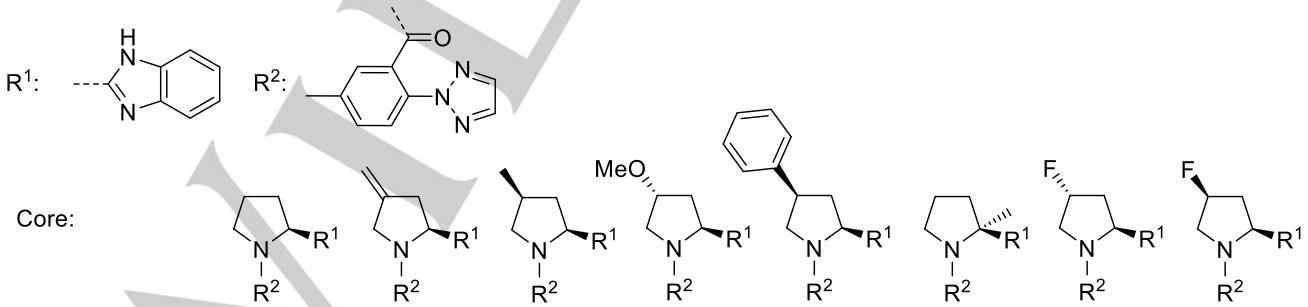

IC_{50}(Ox1 in nM):	2020	2740	2860	1610	1540	280	1980	5430
IC_{50}(Ox2 in nM):	397	286	237	329	619	1010	1080	1840
Compound No.:	**38**	**39**	**40**	**41**	**42**	**43**	**44**	**45**

Figure 8. Substitutions at the pyrrolidine-core.

Table 1. Modification of the benzimidazole substitution pattern

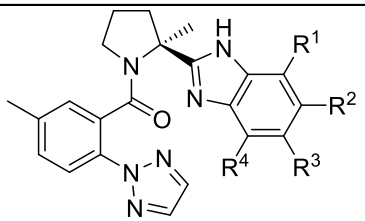

Compound	R^1	R^2	R^3	R^4	IC_{50} hOx1 (nM)[a]	IC_{50} hOx2 (nM)[a]
46	CH_3	H	H	H	19	54
47	H	CH_3	H	H	110	390
48	OCH_3	H	H	H	112	390
49	H	OCH_3	H	H	90	46
50	F	H	H	H	295	2030
51	H	F	H	H	189	931
52	Cl	H	H	H	39	197
53	H	Cl	H	H	29	413
54	Br	H	H	H	23	83
55	H	Br	H	H	13	129
56	CF_3	H	H	H	11	76
57	H	CF_3	H	H	24	129
58	i-Pr	H	H	H	16	47
59	H	t-Bu	H	H	6	30
60	H	SO_2CH_3	H	H	389	1030
61	H	OCF_3	H	H	35	229
62	H	CN	H	H	389	733
63	CH_3	CH_3	H	H	4	19
64	CH_3	F	H	H	19	19
65	CH_3	Cl	H	H	3	10
66	CH_3	Br	H	H	1.7	7
67	F	F	H	H	54	638
68	[b]	[b]	H	H	25	29
69	H	CH_3	CH_3	H	9	19
70	H	F	F	H	40	656
71	H	Cl	Cl	H	3.7	29
72	H	OCH_3	OCH_3	H	31	31
73	H	[c]	[c]	H	515	1270
74	H	F	Cl	H	15	134
75	H	F	Br	H	14	32
76	H	Cl	CH_3	H	6	22
77	H	CF_3	F	H	5	63
78	H	CF_3	Cl	H	1.8	14
79	CH_3	H	CH_3	H	14	19
80	CH_3	H	Br	H	8	14
81	Br	H	F	H	27	81
82	Cl	H	CF_3	H	6	31
83	OCH_3	H	H	OCH_3	44	740
84	CH_3	CH_3	Br	H	0.7	1.4

[a] Data are the geometric mean (+- 2-fold) of at least three independent experiments. [b] Compound **68**: R^1 and R^2 forming a benzodioxane moiety. [c] Compound **73**: R^2 and R^3 forming a benzodioxane moiety.

Larger alkyl substituents in positions 4 or 5, as shown for **58** and **59**, resulted in very interesting potencies on the Ox1R as well as on the Ox2R, asking for further investigations. Introducing a polar substituent in 5-position, such as the methylsulfone group in **60**, yielded generally less active antagonists. The activity of the trifluoromethoxy substituted **61** was comparable to the trifluoromethyl analog **53**. Another polar and electron withdrawing substituent such as nitrile, resulted also in lower orexin receptor antagonist activity (**62**). As a next step, di- and tri-substituted benzimidazoles were prepared and profiled (Compounds **63** to **84**).

The 4,5-dimethyl substitution pattern, as given in **63**, surprisingly resulted in a more active compound as one would expect from the results obtained with **46** and **47**. These results suggested that substituent effects were not purely additive in this series (in both, the positive or negative direction). Fixing the substituent in position 4 to methyl and combining it with a halogen in position 5 (**64** to **66**) resulted in perfect duality in case of fluorine (**64**) and a further gain in potency, especially in case of bromine (**66**). This derivative and the chlorine analog **65** were further characterized and are described in Table 2, Figure 11, and Table 6.

Combining two fluorine substituents (**67**) did not have a similarly beneficial effect as combining two methyl substituents (**63**). Compound **68** bearing a 5,6-dihydro-benzodioxine moiety was a balanced dual orexin receptor antagonist but not attractive enough to be further investigated due to the benzodioxine moiety. The results obtained by putting substituents in positions 5 and 6 are summarized by examples **69** to **78**. Compound **69** exhibited the same orexin receptor antagonist potency as its 3,4-analog **63**. The same was observed for the two bis-fluoro substituted analogs **67** and **70**. Two chlorines (**71**) resulted in better antagonistic activity but an almost 10-fold preference for the Ox1R remained. In case of the 5,6-dihydro-benzodioxine moiety, the analog **73** was significantly less active as compared to **68**. 5,6-dimethoxy-substitution (**72**) resulted in perfect duality with borderline potency. Still compound **72** was further characterized: HLM stability was 186 µL min^{-1} mg^{-1}; P450 inhibition showed IC_{50} values >50 µM for 3A4T, 3A4M, 2C9 and 2D6, and time dependent increase in 3A4 inhibition was > 2.4-fold. The brain penetration experiment performed in rats with sampling 3 h following oral administration of 10 mg kg^{-1}, 30 mg $kg^{-1}$and 100 mg kg^{-1} suggested that **72** was a Pgp substrate in rats. Indeed, the B/P-ratio increased from 13% at 10 mg kg^{-1} ([P]=188 ng mL^{-1}, [B]=26 ng g^{-1}) to 44% at 100 mg kg^{-1} ([P]=11667 ng mL^{-1}, [B]=5060 ng g^{-1}) reflecting a potential saturation of the Pgp with increasing exposure. The efflux ratio in the MDR1 assay with **72** was 49 and the permeability P_{app}AB was 0.9 10^{-6} $cm.s^{-1}$, showing that this compound was in fact also a human Pgp substrate. The compound was abandoned. Compounds **74** to **77** show further substituent combinations in 5,6-positions. These four derivatives showed excellent potency toward the Ox1R and were less potent on the Ox2R, and therefore not further characterized. From the subgroup of 4,6-disubstituted benzimidazole moieties, **78** and **80** turned out to be the most interesting derivatives and are extensively described in Table 2, Figure 11, and Table 6. The 4,7-dimethoxy derivative **83** was not active enough to be further investigated. In contrast, the 4,5-dimethyl-6-bromo substitution pattern (**84**) yielded one of the most potent orexin receptor antagonists identified in this study. Unfortunately, the HLM stability was limited with 266 µL min^{-1} mg^{-1} and the human plasma protein binding was very high with >99.9%. Therefore **84** was as well abandoned.

First *in vitro* characterization of the most interesting compounds **65**, **66**, **78,** and **80** on human and rat liver microsomal stability and P450 inhibition (Table 2) showed acceptable results with HLM between 98 and 206 µL min^{-1} mg^{-1}. The lowest P450 inhibition measured on all 3A4T, 3A4M, 2C9 and 2D6 was with an IC_{50} = 4.5 µM and there was no major time dependent increase in inhibition (max. 2.4-fold). In standard brain penetration experiments where compounds were tested orally at 100 mg kg^{-1}, all 4 compounds showed good exposure (concentration in the brain above 1000 ng mL^{-1}) and brain penetration properties (Brain/Plasma (B/P) ratio between 93% and 185%) at 3h post administration (Table 2).

Table 2. Metabolic stability, cytochrome P450 inhibition and brain penetration properties in rats of **65**, **66**, **78** and **80**.

Parameters	**65**	**66**	**78**	**80**
HLM/RLM clearance in µL min^{-1} mg^{-1}	206 / >1250	186 / 947	98 / 276	155 / 879
3A4T in µM	11	11	7.9	8.4
3A4 shift	2.4	1.7	2.1	2
3A4M in µM	12	17	>50	17
2C9 in µM	7.2	13	4.5	5.7
2D6 in µM	39	39	13	33
Brain penetration experiments in rats at 100 / 30 mg kg^{-1}, 3h post administration [a]				
[plasma] [b] in ng mL^{-1}	1219 ± 142 / 125 ± 48	1677 ± 253 / nd	2513 ± 770 / 1190 ± 313	2095 ± 234 / 723 ± 108
[brain] [b] in ng g^{-1}	2201 ± 221 / 145 ± 47	2379 ± 561 / nd	2348 ± 478 / 1632 ± 608	3880 ± 1362 / 753 ± 144
B/P ratio	181 / 117	142 / nd	93 / 137	185 / 104
[CSF] [c] in ng mL^{-1}	50 ± 3 / 3 ± 3	49 / nd	58 ± 27 / 28	49 ± 1 / 14 ± 5

[a] formulated in 100 % PEG400. [b] values given as mean ± SEM of n=3. [c] values for n=1-3; nd: not determined

These compounds were pursued and tested in freely moving male Wistar rats implanted with telemetry devices to continuously record EEG/EMG as previously described. [38] First compounds to be tested were **65** and **80**. Our initial approach was to test compounds orally at 100 mg kg^{-1} in a polyethylene glycol 400 (PEG400) formulation and, if efficacy was observed, to decrease the dose to 30 mg kg^{-1}. At 100 mg kg^{-1}, over the 12 h night period following administration, compounds **65** and **80** increased significantly the time spent in NREM sleep by 29 min (p=0.0011) and by 37 min (p=0.0004), respectively (Figure 9) compared to matched vehicle. Both also increased the time spent in REM sleep (+9 min and +30 min respectively), although statistically significantly only for **80** (p=0.0082). At 30 mg kg^{-1}, a similar pattern was seen with a significant increase of the time spent in NREM sleep of 17 min and 35 min for **65** (p=0.0448) and **80** (p=0.0051),

respectively and a significant increase of REM sleep time for **80** (+13 min, p=0.0332) (Figure 9). Because efficacy was observed at 30 mg kg^{-1} for both compounds, we decided to change our starting dose for *in vivo* testing in EEG/EMG from 100 mg kg^{-1} to 30 mg kg^{-1}.

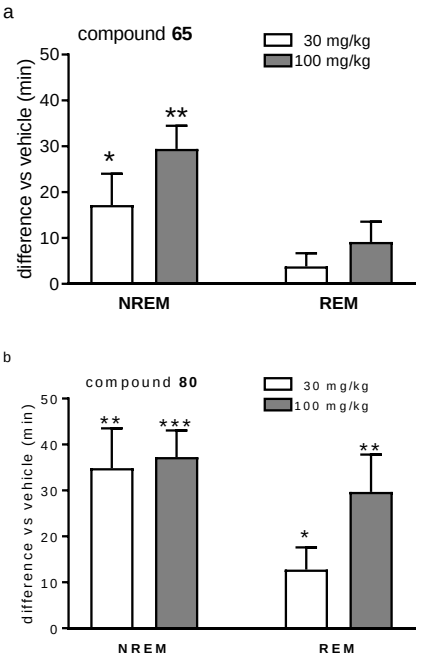

Figure 9. Effect of 30 and 100 mg kg^{-1} oral administration of **65** and **80** on sleep stages. Summary of the 12 h night active period following oral administration of compound **65**, a) and compound **80**, b) formulated in 100% PEG400. Data are expressed as mean ± SEM. *p<0.05, **p<0.01, ***p<0.001 vs matched vehicle, paired t-test. n=7-8 per group. REM, rapid eye movement; NREM, non-REM.

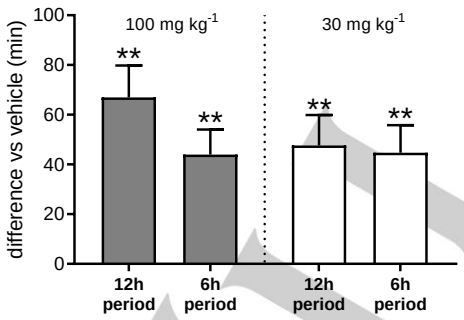

Figure 10. Effect of **80** on total sleep time. Summary of the 6 or 12 h night active period following oral administration of compound **80** formulated in 100% PEG400. Data are expressed as mean ± SEM. **p<0.01vs matched vehicle, paired t-test. n=7-8 per group. REM, rapid eye movement; NREM, non-REM.

In addition, as expected with compound **80** (Figure 10), by decreasing the dose, the duration of action decreased. Whereas at 100 mg kg^{-1}, a larger increase in sleeping time was seen when looking at the data over the 12 h period (+67 min vs vehicle) compared to the 6 h period (+44 min), at 30 mg kg^{-1}, a very similar increase was seen (+48 and +45 min vs vehicle for the 12h and 6h period analysis, respectively). It suggested that the evaluation and comparison of the subsequent compounds could be performed at 30 mg kg^{-1} over the 6h period following administration.

In this first series, all 4 compounds (**65**, **80**, **66** and **78**) significantly increased the time spent sleeping following administration of 30 mg kg^{-1}, from 22 min (compound **65)** to 45 min (compound **80**) (Figure 11). Compound **80** showed the largest increases in NREM sleep (+31 min vs vehicle) whereas compound **78** had limited efficacy on NREM sleep (+13 min vs vehicle).

The next step was the optimization of the amide substituent with a few selected benzimidazoles. Results are summarized in Table 3**Error! Reference source not found.**. For this investigation and based on previous *in vivo* results, we had selected the 4-methyl-5-chloro-, the 5-trifluoromethyl-6-chloro-, the 5,6-dimethoxy- and the 5-trifluoromethoxy-substitution patterns on the benzimidazole part and combined them with a series of bi-aryl-carboxylic acid derivatives with a focus on 2-triazolo substitution combined with one or two additional substituents on the phenyl ring.

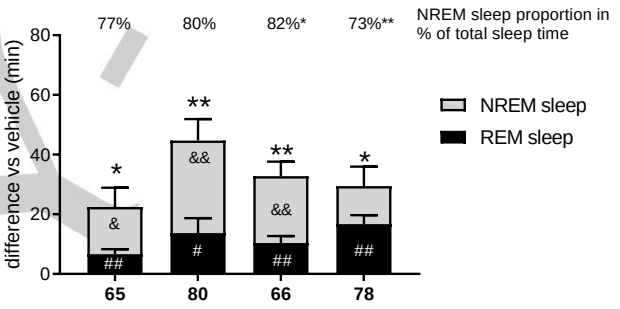

Figure 11. Effect of 30 mg kg^{-1} of **65**, **80**, **66**, and **78** on sleep stages. Summary of the 6 h night active period following oral administration of compounds formulated in 100% PEG400. Data are expressed as mean ± SEM. n=7-8 per group. NREM sleep proportion is given for the compound treated group. REM, rapid eye movement; NREM, non-REM. For total sleep time: *p<0.05, **p<0.01; for NREM sleep: &p<0.05, &&p<0.01; for REM sleep: #p<0.05, ##p<0.01 each vs matched vehicle, paired t-test.

In the group of compounds **85** to **88**, wherein the 2-triazolo-5-methyl-benzoyl moiety was replaced by a 2-triazolo-5-fluoro-benzoyl moiety, **85** (containing the 4-methyl-5-chloro pattern on the benzimidazole part), was clearly the most potent dual orexin receptor antagonist and was further characterized as described in Table 4, Figure 12 and Table 6 together with all the most interesting compounds from Table 3. In the following group bearing the 2-triazolo-5-chloro-benzoyl substituent, **92** was abandoned due to low antagonist potency, and **90** because of its preferential activity towards the Ox1R. Compound **89** which is again the combination with the 4-methyl-5-chloro pattern in the benzimidazole part was further characterized. Compound **91** was further characterized in vitro. Stability in HLM was 90 µL min^{-1} mg^{-1}; P450 inhibition was 3A4T IC_{50} = 41 µM; 2C9 IC_{50} >50 µM; 2D6 IC_{50} >50 µM and time dependent increase in 3A4 inhibition was > 2.7-fold. In the *in vivo* brain penetration -experiment at 100 mg kg^{-1} p.o., plasma and brain exposure were very high at 3h post administration with 16907 ng mL^{-1} and 18827 ng g^{-1}, respectively,

Table 3. Best benzimidazoles R^1 combined with a set of benzoic acids as R^2

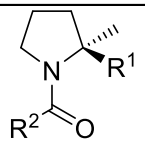

		IC_{50} (Ox1) in nM [a] IC_{50} (Ox2) in nM [a] **Cmpd No**				
R^2	**R^1**	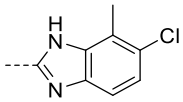	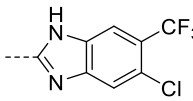	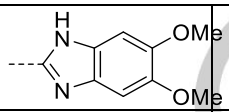	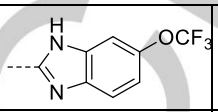	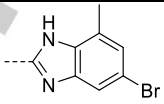
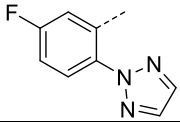		4.9 13 **85**	5.6 34 **86**	200 154 **87**	138 720 **88**	N.D.
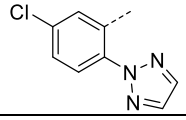		3 8 **89**	2.3 21 **90**	10 23 **91**	99 119 **92**	N.D.
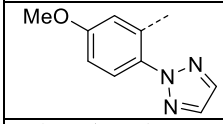		1.4 3.2 **93**	N.D.	25 26 **94**	46 199 **95**	N.D.
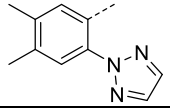		1.9 3.1 **96**	1.5 4.5 **97**	15 25 **98**	5 16.5 **99**	N.D.
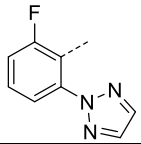		12 25 **100**	11 45 **101**	872 458 **102**	529 1600 **103**	N.D.
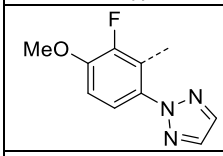		10 13 **104**	8.9 36 **105**	414 1200 **106**	197 1870 **107**	N.D.
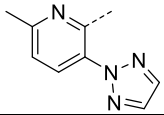		2.5 10 **108**	5.6 25 **109**	316 114 **110**	N.D.	N.D.
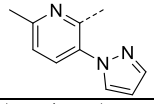		5.6 31 **111**	7.3 82 **112**	426 104 **113**	N.D.	N.D.
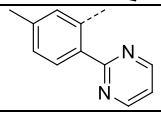		3.6 7.6 **114**	3 7.8 **115**	36 16 **116**	34 380 **117**	6 13 **118**

[a] Data are the geometric mean (+- 2-fold) of at least three independent experiments.

resulting in a B/P-ratio of 111%. However, the efflux ratio of 25 and the $P_{app}AB$ of 2.5 10^{-6} $cm.s^{-1}$ in the MDR-1 assay, showed that this compound was a Pgp substrate in human, confirming the high likelihood of compounds combining two aromatic methoxy-substituents of being human Pgp substrates, as previously observed with **72**. Compound **91** was therefore discarded. In the next group containing the 2-triazolo-5-methoxy-benzoyl substituent, **95** was not further characterized due to its relatively low potency. Compound **93 (ACT-541468, Daridorexant)**, again part of the 4-methyl-5-chloro-benzimidazole subgroup was very promising and was further characterized. The remaining compound **94** was further characterized since the 5,6-dimethoxy-benzimidazole moiety resulted, so far, always in very good exposure data in the rat. This was also true for this compound. The *in vivo* brain penetration -experiment performed at 100 mg kg^{-1} p.o. in rats resulted, 3h post administration, in the highest exposure seen during the project so far, with plasma concentration of 35640 ng mL^{-1} but a brain concentration of 11673

ng g^{-1}, giving a B/P ratio of only 33%. This nurtured the suspicion that, as previously seen in 5,6-dimethoxy-benzimidazole containing compounds, **94** was a Pgp-substrate also in human. Indeed, in the MDR-1 assay the efflux ratio was 63 and $P_{app}AB$ was 0.8 10^{-6} cm.s^{-1}, and as a result **94** was not further investigated. Otherwise **94** was very stable in HLM with 14 µL min^{-1} mg^{-1} and the IC_{50} values for all P450 investigated were > 50 µM. The introduction of the 2-triazolo-4,5-dimethyl-benzoyl moiety resulted in a subgroup **96** to **99**, all exhibiting very good antagonist potency on both the Ox1R and the Ox2R. Compound **99** showed a decent HLM stability of 205 µL min^{-1} mg^{-1} and 3A4T inhibition of 26 µM. The 5,6-dimethoxy-benzimidazole derivative **98** resulted in HLM stability of 39 µL min^{-1} mg^{-1}, did not inhibit any of the P450 measured (IC_{50} > 50 µM), but showed a time dependent increase in inhibition of 3A4 > 9. It was therefore stopped. The 5-trifluoromethyl-6-chloro-benzimidazole derivative **97** showed very promising dual orexin antagonistic activity and was further characterized. Compound **96**, the 4-methyl-5-chloro-benzimidazole derivative resulted in HLM stability of 456 µL min^{-1} mg^{-1} and the 3A4T inhibition was at 6.8 µM. In the *in vivo* brain penetration experiment in rats at 100 mg kg^{-1}, the compound could neither be detected in plasma nor in the brain 3h post administration. The results of the MDR1 assay did not highlight a major Pgp issue for human with an efflux ratio of 3.4 and $P_{app}AB$ of 19.10^{-6} cm.s^{-1}. This result indicated how subtle structural changes can influence PK behavior. The next subgroup of compounds containing the 2-triazolo-6-fluoro-benzoyl substituent **100** to **103** showed less antagonist potency on the Ox2R and was not further characterized. Adding a methoxy group to obtain the 2-triazolo-5-methoxy-6-fluoro-benzoyl moiety, resulted in compounds **104** to **107**. The derivatives **106** and **107** exhibited low orexin receptor antagonist potency and were not further characterized. The 5-trifluoromethyl-6-chloro-benzimidazole derivative **105** showed good HLM stability (48 µL min^{-1} mg^{-1}) and P450 inhibition in the 3A4T assay was 6.5 µM. The 4-methyl-5-chloro-benzimidazole member of this subgroup (**104**) resulted in interesting antagonist potency on both orexin receptors and was further characterized. As a next investigation, the phenyl ring of the benzoyl substituents was changed into a pyridine ring, resulting in the 6-methyl-3-triazolyl-2-picolinoyl unit reflected in **108** to **110**. The results obtained in combination with the 4-methyl-5-chloro-benzimidazole unit (**108**) were very interesting and also this compound was further characterized. Compound **109** exhibited interesting receptor potency, was very stable in HLM (12 µLmin^{-1} mg^{-1})), and showed a reasonable P450 inhibition profile with 3A4T IC_{50}= 9.9 µM, 2C9 IC_{50}= 4.5 µM and 2D6 IC_{50}= 23 µM. No time dependent increase in P450 inhibition was detected. The compound was abandoned for further characterization as it was a Pgp-substrate (Efflux ratio = 5.9; PappAB = 8.2 10^{-6} cm.s^{-1}). Compound **110** was as well not further investigated as it was not potent enough on the orexin receptors. Combining the pyridine ring with a pyrazole substituent resulted in **111** to **113** containing a 6-methyl-3-pyrazolyl-picolinyl substituent. Again, the combination with the 4-methyl-5-chloro-benzimidazole moiety resulted in the very promising compound **111** which will be discussed in detail. Based on the Ox2R potency, **112** and **113** were not further characterized. The last group of compounds **114** to **118** contain a 5-methyl-2-pyrimidinyl-benzoyl moiety attached to the proline ring nitrogen. Compounds **114** and **118**, both very potent dual orexin receptor antagonists, were further characterized. Compound **116** was not further characterized under the assumption it was a strong Pgp-substrate as the other derivatives from the 5,6-dimethoxy-benzimidazole sub-series. Compound **117** was abandoned based on its low orexin receptor antagonist potency. In this investigation we found that the 4-methyl-5-chloro-benzimidazole unit resulted in the most promising dual orexin receptor antagonists in combination with various substituents attached by an amide bond to the pyrrolidine ring-nitrogen atom of the template.

Table 4. Metabolic stability, cytochrome P450 inhibition and brain penetration properties in rats of the most interesting compounds from Table 3

Parameters	**85**	**89**	**93**	**97**	**104**	**108**	**111**	**114**	**118**
HLM/RLM clearance in µL min^{-1} mg^{-1}	96 / >1250	125 / 645	138 / 990	197 / 618	64 / 1180	111 / 437	106 / 572	138 / >1250	69 / 988
3A4T in µM	5.6	6.2	4.1	6.1	8.4	16	15	12	18
3A4 shift	1.3	1.3	2.1	1.9	2.1	> 1.7	1.2	1.5	2.1
3A4M in µM	3.6	8.5	7.3	> 50	14	11	12	28	41
2C9 in µM	8.1	5.5	14	5.7	7.7	24	30	19	7.5
2D6 in µM	33	23	31	21	30	> 50	>50	> 50	29
Brain penetration experiments in rats at 100 / 30 mg kg^{-1}, 3h post administration [a]									
[plasma][b] in ng mL^{-1}	1354 ±152 / nd	1205 ±307 / 273 ± 63	1280 ± 31 / 309 ± 42	786 ±220 / 321 ± 31	1144 ± 60 / nd	2029 ± 513 / 520 ± 135	9816 ± 2244 / 371 ± 95	1087 ± 103 / 236 ± 21	3560 ± 602 / 513 ± 65
[brain][b] in ng g^{-1}	3507 ± 1133 / nd	2895 ± 595 / 536 ± 136	1808 ± 116 / 300 ± 63	1537 ±471 / 495 ± 37	1984 ± 256 / nd	1999 ± 685 / 293 ± 100	13005 ± 4455/ 97 ± 33	2230 ± 265 / 153 ± 12	5880 ± 1201 / 301 ± 34
B/P ratio	259 / nd	240 / 196	141 / 97	196 / 154	173 / nd	99 / 56	132 / 26	205 / 65	165 / 59
[CSF] [c] in ng mL^{-1}	118 ± 36 / nd	30 ± 5 / 5 ± 3	63 ±3 / 24 ± 5	10 ± 5 / 6 ± 2	49 ± 4 / nd	242 ± 63 / 27	1862 / 7.2 ± 0.2	54 ± 7 / 25 ± 1	105 ± 37 / 10

[a] formulated in 100 % PEG400. [b] values given as mean ± SEM of n=3. [c] values for n=1-3. nd: not determined.

First *in vitro* characterization of the most interesting compounds, summarized in Table 4, were performed on human and rat liver microsomal stability and P450 inhibition.

All compounds showed results on HLM between 64 and 197 µL min^{-1} mg^{-1} and lowest P450 inhibition on all 3A4T, 3A4M, 2C9 and 2D6 at 3.6 µM with no time dependent inhibition of 3A4 (max. 2.1-fold). In standard brain penetration experiments, where compounds were tested orally at 100 mg kg^{-1}, all 4 compounds showed good exposure (concentration in the brain above 1500 ng mL^{-1}) and brain penetration properties (B/P ratio between 99 and 259%) at 3h post administration (Table 4).

When tested in an EEG experiment at 30 mg kg^{-1} (Figure 12), **85**, **89** and **111** showed a trend but no statistically significant increase of the time spent in NREM (+7 to +12 min depending on compounds) and REM sleep (+4 to +8 min) over the 6h period following administration. This trend translated to a statistically significant increase of the total time spent asleep for compound **111** only (+15 min of sleep vs vehicle). All the other compounds (**93**, **97**, **104**, **114** and **118**) showed statistically significant increases of the time spent sleeping (from +25min for compound **104** to +53 min for compound 1**08** (vs vehicle)) with a significant increase of the time spent in NREM sleep (from +15 min for compound **97** to +34 min for compound **108**). In the 5 compounds, only compound **104** did not increase in a statistically significant manner the time spent in REM sleep (+10 min vs vehicle).

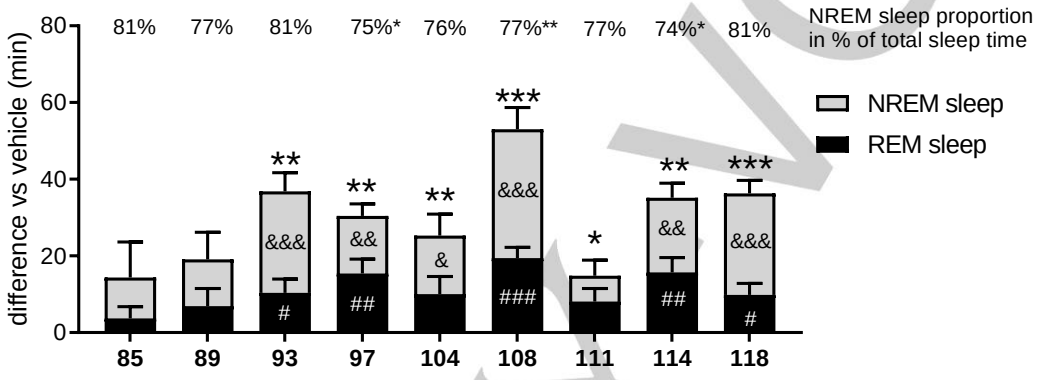

Figure 12. Effect of 30 mg kg^{-1} of **85**, **89**, **93**, **97**, **104**, **108**, **111**, **114**, and **118** on sleep stages. Summary of the 6 h night active period following oral administration of compounds formulated in 100% PEG400. Data are expressed as mean ± SEM. n=7-8 per group. NREM sleep proportion is given for the compound treated group. REM, rapid eye movement; NREM, non-REM. For total sleep time: *p<0.05, **p<0.01, ***p<0.001; for NREM sleep: &p<0.05, &&p<0.01, &&&p<0.001; for REM sleep: #p<0.05, ##p<0.01, ###p<0.001 each vs matched vehicle, paired t-test.

Based on the very interesting results obtained in the profiling of **93** (see Table 4, Figure 12, and Table 6), it was decided to investigate a few additional benzimidazole substitution patterns in combination with the 2-triazolo-5-methoxy-benzoyl moiety attached via an amide linkage to the template ring nitrogen atom. The results are depicted in Figure 13. All the compounds **119** to **123** showed decent potency, especially **119** and **120**, wherein the chloro substituent attached to the 5-position of the benzimidazole system was replaced by bromo or fluoro, respectively. Methylation at the benzimidazole moiety resulted in the very potent dual orexin antagonist **123**. By NMR-experiments, it was shown that methylation or alkylation (see Figure 16) predominantly results in the drawn regioisomer. Due to their lower orexin receptor antagonist potency, **121** and **122** were not further characterized. Compound **119** was further characterized and is discussed in detail in Table 5, Figure 14, and Table 6. Further characterization of **120** resulted in good HLM stability of 71 µL min^{-1} mg^{-1}), human PPB of 99.8% and an efflux ratio in the MDR1 assay of 4 with a permeability $P_{app}AB$ of 14 10^{-6} $cm.s^{-1}$. With this efflux ratio and because we had compounds with overall better profile, the further evaluation of **120** was stopped. This targeted investigation confirmed that the 4-methyl-5-chloro-pattern was the best choice on the benzimidazole unit when combined with the 2-triazolo-5-methoxy-benzoyl moiety.

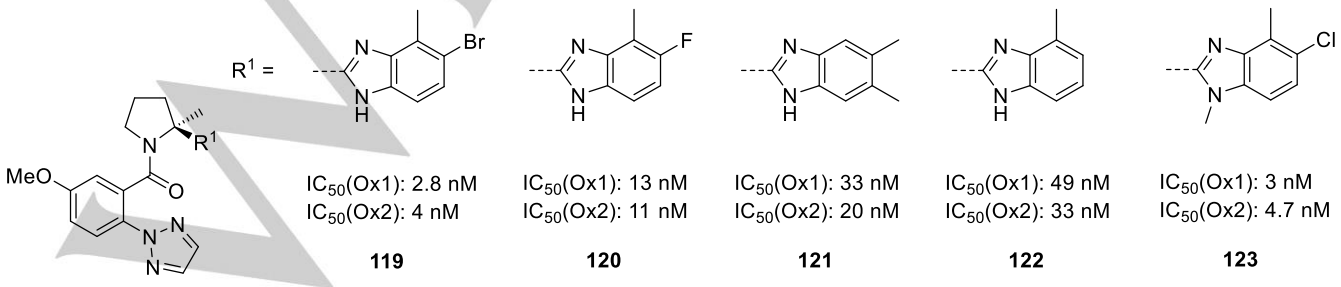

Figure 13. Further substituent variations in combination with «triazolo-methoxy-benzoic acid».

Table 5. Metabolic stability, cytochrome P450 inhibition and brain penetration properties in rats of compounds **119** and **139**

Parameters	**119**	**139**
HLM/RLM clearance in µL min^{-1} mg^{-1}	134 / 658	149 / 835
3A4T in µM	5.8	8.9
3A4 shift	1.4	2.9
3A4M in µM	10	4.4
2C9 in µM	15	30
2D6 in µM	> 50	50
Brain penetration experiment in rats at 100 / 30 mg kg^{-1}, 3h post administration [a]		
[plasma][b] in ng mL^{-1}	2196 ± 139 / nd	823 ± 73 / 222 ± 51
[brain][b] in ng g^{-1}	3173 ± 476 / nd	1009 ± 45 / 69 ± 31
B/P ratio	145	123 /31
[CSF] [c] in ng mL^{-1}	66 ± 13 / nd	42 / 1.4 ± 1.4

[a] formulated in 100 % PEG400. [b] values given as mean ± SEM of n=3-4. [c] values for n=1-4. nd: not determined.

Compound **119**, the only compound further characterized from Figure 13 showed an HLM stability at 134 µL min^{-1} mg^{-1}. P450 inhibition was acceptable and in the brain penetration experiment at the dose of 100 mg kg^{-1} the compound showed good brain penetration properties (Table 5). However, when tested in the EEG experiment at 30 mg kg^{-1}, the sleep promoting effect was limited with no significant increase of the total sleep time (+19 min vs vehicle), NREM (+12 min) or REM (+ 7 min)) (Figure 14).

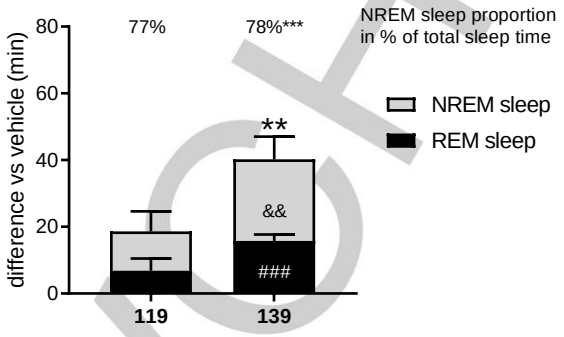

Figure 14. Effect of 30 mg kg^{-1} of compounds **119** and **139** on sleep stages. Summary of the 6 h night active period following oral administration of compound formulated in 100% PEG400. Data are expressed as mean ± SEM. n=8. NREM sleep proportion is given for the compound treated group. REM, rapid eye movement; NREM, non-REM. For total sleep time: **p<0.01; for NREM sleep: $^{\&\&}$p<0.01; for REM sleep: $^{\#\#\#}$p<0.001 each vs matched vehicle, paired t-test.

In Figure 15 we summarize further modifications of the carboxylic acid moieties in combination with the 4-methyl-5-chloro-benzimidazole.

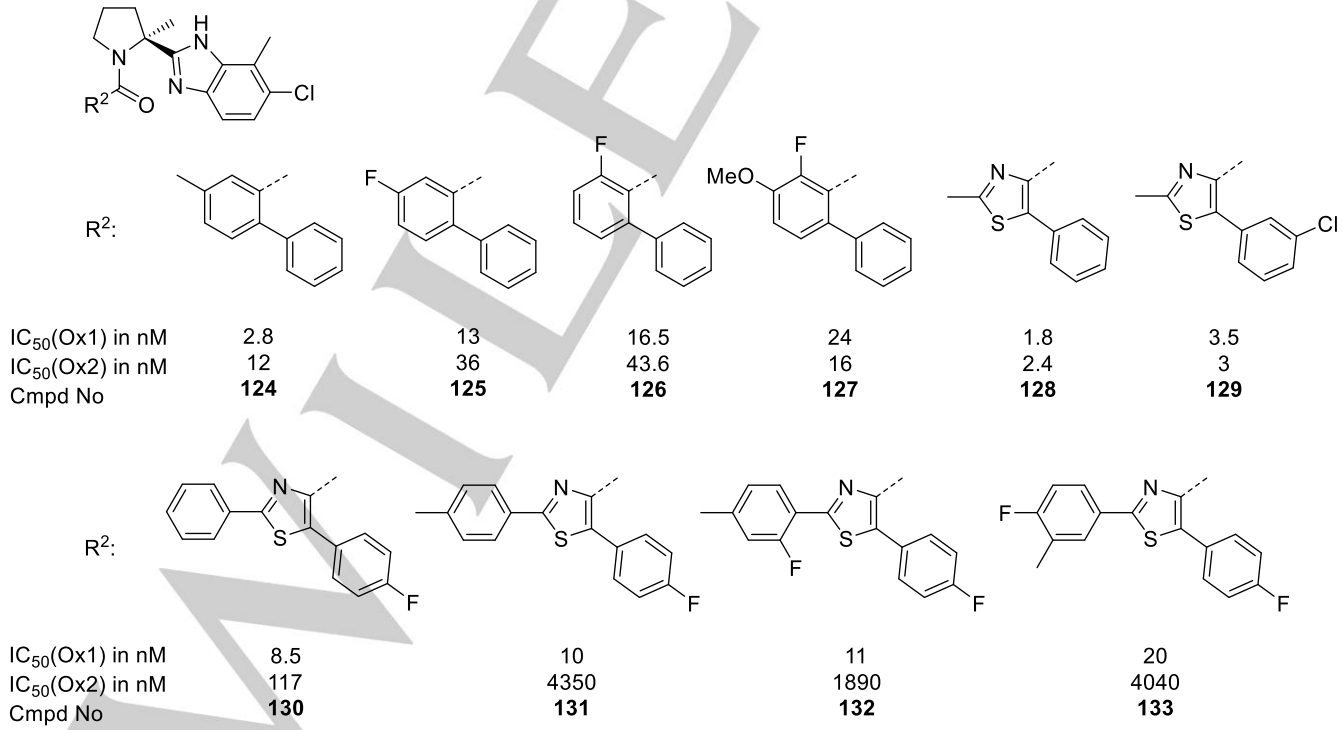

Figure 15. Further exploration of benzoic- and heteroaryl carboxylic acid moieties in combination with the 4-methyl-5-chloro-benzimidazole

First, we investigated substituted biphenyl groups as benzoyl-substituents. Orexin antagonist activities, especially on the Ox2R, showed a tendency towards weaker potency. Human liver microsomal stabilities of 116 µL min^{-1} mg^{-1} and 103 µL min^{-1} mg^{-1} were determined for **124** and **125**, respectively. P450 inhibition in the 3A4T assay resulted in IC_{50} of 3.6 µM and 2.3 µM for **124** and **125**, respectively. This, combined with the suboptimal Ox2R antagonist activity, resulted in the decision to stop further work with these compounds. Compound **126** did not show sufficient orexin receptor antagonist potency to be of further interest. Compound **127** showed HLM stability of 194 µL min^{-1} mg^{-1}. In the P450 assays, IC_{50} values were 7 µM for 3A4T, 2.6 µM for 2C9 and 6.6 µM for 2D6. Unfortunately, the time dependent increase in 3A4 inhibition was very high with 23-fold. The 5-phenyl-thiazoloyl derivative **128** was a very potent DORA with HLM stability of 296 µL min^{-1} mg^{-1}. For this compound, the P450 inhibition assays resulted in IC_{50} of 6.2 µM for 3A4T, 6.3 µM for 2C9 and 12 µM for 2D6. Unfortunately, here as well, the time dependent increase in 3A4 inhibition was very high with 12.8-fold. Another potent DORA was **129** with an additional chloro-substituent on the phenyl ring. Human liver microsomal stability was 285 µL min^{-1} mg^{-1}, P450 inhibition was at the lower, acceptable end (3A4T IC_{50} = 4.2 µM; 3A4M IC_{50}= 14 µM; 2C9 IC_{50}= 4.8 µM; 2D6 IC_{50} = 13 µM) and time dependent increase in 3A4 inhibition resulted in 2.9-fold. In the *in vivo* brain penetration -experiment at 100 mg kg^{-1}, plasma concentrations of 558 ng mL^{-1} and brain concentrations of 607 ng g^{-1} were observed 3h post administration, resulting in a B/P-ratio of 109%. Because of the relatively limited exposure compared to other compounds tested up to now, this compound was tested at 100 mg kg^{-1} p.o. to assess its sleep promotion potential in rats. Compound **129** increased the time spent in NREM sleep by 29 ± 12 and in REM sleep by 17 ± 4 min over the 12h post administration period. However, statistical significance was reached only for REM sleep (p = 0.0520 and p = 0.0039 compared to vehicle for NREM and REM sleep, respectively, paired t-test). In addition, it showed a very high human plasma protein binding of >99.9%.

Compounds **130** to **133**, containing a 2,5-diphenyl-thiazol-4-oyl substituent, represent rather Ox1R preferential or selective antagonists. Therefore, these compounds were not further characterized in this study.

In Figure 16, a summary of selected N-alkylated benzimidazoles is depicted. Based on its very good dual orexin receptor antagonist potency, **134** was further characterized. HLM stability resulted in 99 µL min^{-1} mg^{-1}. P450 inhibition was acceptable (3A4T IC_{50} = 9.1 µM; 3A4M IC_{50} = 12 µM; 2C9 IC_{50} = 17 µM; 2D6 IC_{50} = 49 µM) and time dependent increase in 3A4 inhibition was 1.7-fold. In the *in vivo* brain penetration experiment at 100 mg kg^{-1} p.o., plasma concentrations were 1303 ng mL^{-1} and brain concentrations 508 ng g^{-1} (ratio of 39%) indicating the potential of this compound being a Pgp-substrate. In addition, human PPB was > 99.9%.

Compounds **135** to **138** were not further characterized due to limited orexin receptor antagonist potency. Compound **140**, a highly potent DORA resulted in an inacceptable time dependent increase of 3A4-inhibition of 5 and was therefore abandoned as well.

Finally, compound **139** (Figure 16), showed an HLM stability at 149 µL min^{-1} mg^{-1}. P450 inhibition was acceptable and the *in vivo* brain penetration experiment at the dose of 100 mg kg^{-1} resulted in good brain penetration properties (Table 5). When tested at 30 mg kg^{-1} in the EEG experiment, **139** significantly increased the total sleep time (+ 40 min vs vehicle) via an increase of 24 min of NREM sleep and 16 min REM sleep (Figure 14).

Out of the investigations summarized so far, the interesting "*15 good compounds*" which were investigated in the EEG/EMG experiment at 30 mg kg^{-1} were further characterized in order to select the best one for preclinical and clinical development.

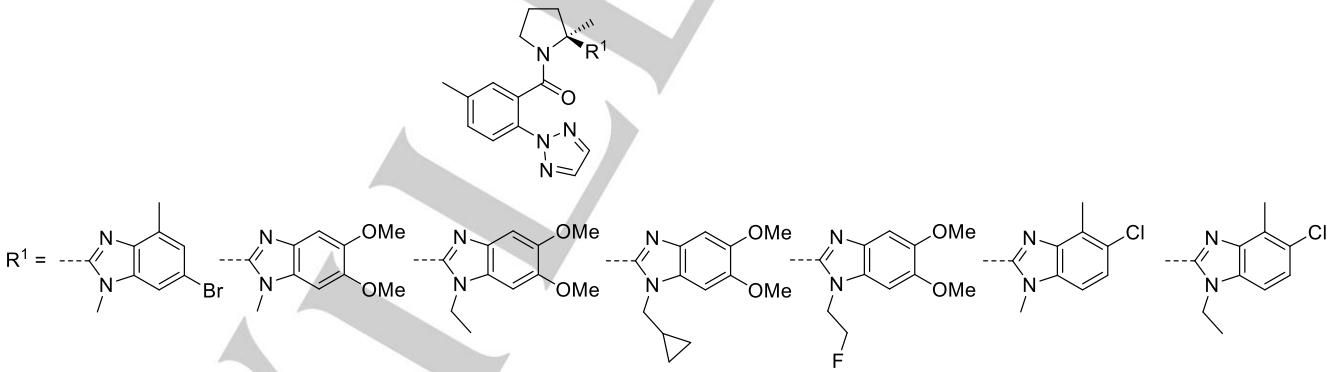

	134	135	136	137	138	139	140
IC_{50}(Ox1)	7.1 nM	28 nM	33 nM	40 nM	33 nM	1.1 nM	1.1 nM
IC_{50}(Ox2)	5.5 nM	28 nM	42 nM	60 nM	40 nM	1.2 nM	1.2 nM

Figure 16. N-alkylated benzimidazoles (see also cpd 118).

Whereas many compounds showed promising *in vivo* efficacy in rats, the overall profile of the compounds was looked at to select the most promising drug candidate for clinical development. Physiology-based pharmacokinetic and pharmacodynamic (PBPK/PD) modeling was then used to identify those compounds with the best PK/PD profile in man. [1]

Table 6. The 15 compounds investigated for their sleep promotion potential in rats

Parameters	65	66	78	80	85	89	93	97
Kb hOx1R / Kb hOx2R in nM	0.8 / 1.1	0.5 / 1	3.1 / 2.8	8.8 / 13	2.5 / 3.5	1.1 / 1.6	0.7 / 1.2	3.4 / 5.4
[a] Increase in total sleep time in min	22	33**	29*	45**	14	19	37**	30** *
MDR1 assay: Efflux $P_{app}AB$ in 10^{-6} cm.s^{-1}	2.7 21	3.4 16	2.3 28	2.2 31	2.1 30	2.3 33	3.3 24	2.3 18
PPB in % Human / Rat / Dog	99.94 / 99.4 / 99.6	>99.9 / 99.2 /99.5	99.92 / 99.6 / 99.6	99.8 / 99.3 / 99.7	99.6 / 99.2 / 99.7	99.92 / 99.4 / 99.7	99.9 / 98.3 / 99.4	>99.9 / 99.8
hPXR activation: EC_{50} in µM E_{max} in %	3.6 5.3	2.3 3.3	1.6 6	3.5 5.4	1.8 7.1	1.9 7	4 5.2	0.7 9.7
Stability in liver microsomes in µL min^{-1} mg^{-1} Human / Rat / Dog	206 / >1250 / 335	186 / 947 / 267	98 / 276 / 55	155 / 879 / 80	96 / >1250 / 88	125 / 645 / 87	138 / 990 / 235	197 / 618 / n.d.
i.v. PK in rat: 1 mg kg^{-1} AUC in ng*h/mL CL in mL/(min*kg) Vss in L/kg $T_{1/2}$ in h	325 51 3.8 3.2	113 150 7.9 0.9	461 36 11 6.2	498 33 2.2 2.2	Not performed based on EEG inactivity	553 30 3.6 2.7	196 85 3.9 1.3	n.d.
[b] **oral PK in rat: 10 mg kg^{-1}** C_{max} in ng mL^{-1} T_{max} in h AUC in ng*h/mL F in %	126 0.5 208 6.4	261 0.5 240	319 0.5 1590 34	400 0.5 562 11.3	Not performed based on EEG inactivity	415 0.5 592 11	174 0.5 186 9.4	n.d.
i.v. PK in dog: 1 mg kg^{-1} AUC in ng*h/mL CL in mL/(min*kg) Vss in L/kg $T_{1/2}$ in h	1690 9.9 3.7 6.5	1500 11 2.5 5.4	2070 8.1 5 9.7	1930 8.6 3.6 6.4	Not performed based on EEG inactivity	1160 14 5.4 6.8	1750 9.5 2.4 5	n.d.
[b] **oral PK in dog: 30 mg/dog** C_{max} in ng mL^{-1} T_{max} in h AUC in ng*h/mL F in %	247 0.3 1090 38	278 0.5 690 23	68 2 626 20	384 0.3 1560 42	Not performed based on EEG inactivity	85 1.0 355 17	239 1 910 35	n.d
Brain Fu in %	0.7	0.3	0.2	0.5	0.9	0.3	1	1.1

[a] 30 mg kg^{-1} p.o. formulated in 100% PEG400. [b] formulated in MC0.5%. *p<0.05, **p<0.01, ***p<0.001 vs matched vehicle, hPXR: human pregnane X receptor, n.d.: not determined

Table 6. continued

Parameters	104	108	111	114	119	118	139
Kb hOx1R / Kb hOx2R in nM	5.2 / 8.1	4.0 / 4.6	3.8 / 4.5	7.7 / 1.9	1.2 / 1.4	1.6 / 5.5	1.0 / 1.9
[a] Increase in total sleep time in min	25**	53***	15*	35**	19	36***	40**
MDR1 assay:							
Efflux	2.9	8.4	13	2.5	2.2	1.4	4.7
$P_{app}AB$ in 10^{-6} cm.s^{-1}	16	9.7	4.5	28	23	34	20
PPB in % Human / Rat / Dog	99.6 / 98.2 / 99.4	99.7 / 97.3 / 97.5	99.8 / 97.2 / 98.6	>99.9 / 98.8 / 99.2	>99.9 / 98.8 / 99.2	99.2 / 99.1 / 99.2	99.97 / 98.7 / 98.9
hPXR activation:							
EC_{50} in µM	2.6	2.3	1.6	1.9	0.9	0.4	4.6
E_{max} in %	5.1	5.2	6.7	7.1	4.1	4	5.5
Stability in liver microsomes in µL min^{-1} mg^{-1} Human / Rat / Dog	64 / 1180 / 156	111 / 437 / 65	106 / 572 / 68	138 / >1250 / 182	134 / 658 / 185	69 / 988 / 89	149 / 835 / 212
i.v. PK in rat: 1 mg kg^{-1}							
AUC in ng*h/mL	n.d.	767	n.d.	616	n.d.	461	524
CL in mL/(min*kg)		22		27		36	32
Vss in L/kg		0.6		1.2		3.2	0.79
$T_{1/2}$ in h		0.4		1.3		1.7	0.4
[b] **oral PK in rat: 10 mg kg^{-1}**					[#]		
C_{max} in ng mL^{-1}	n.d.	846	n.d.	464	121	1050	346
T_{max} in h		0.3		0.3	0.5	0.5	1.0
AUC in ng*h/mL		1170		965	212	1900	911
F in %		15		16	n.a.	43	?
i.v. PK in dog: 1 mg kg^{-1}							
AUC in ng*h/mL	n.d.	1900	n.d.	2160	n.d.	4220	2260
CL in mL/(min*kg)		8.8		7.7		3.9	7.4
Vss in L/kg		1.2		2.5		2.2	1.1
$T_{1/2}$ in h		1.5		5.5		8.5	2.9
[b] **oral PK in dog: 30 mg/dog**							
C_{max} in ng mL^{-1}	n.d.	747	n.d.	211	n.d.	736	774
T_{max} in h		0.3		0.8		0.25	0.5
AUC in ng*h/mL		1620		818		2750	2130
F in %		49		20		39	28
Brain Fu in %	1.1	3	2.5	0.8	n.d.	0.7	0.8

[a] 30 mg kg^{-1} p.o. formulated in 100% PEG400. [b] formulated in MC0.5%. *p<0.05, **p<0.01, ***p<0.001 vs matched vehicle, hPXR: human pregnane X receptor, n.d.: not determined, [#] formulated in 100% PEG400

Based on limited efficacy on either total sleep time, NREM sleep or REM sleep time at 30 mg kg-1 compared to the other compounds, **78**, **85**, **89**, **104**, **111,** and **119** were discarded. The lack of efficacy of **111** was associated with a strong decrease of exposure and a decrease in B/P ratio in the brain penetration experiment when decreasing the dose from 100 to 30 mg kg^{-1}, suggesting this compound could be a Pgp substrate in rats. Looking at the MDR1 data, **111** was a clear Pgp substrate in human with an efflux ratio of 13. Compound **108** was also classified as a Pgp substrate in human based on the MDR1 data showing an efflux ratio of 8.4 and was discarded. **139**, with is efflux ratio of 4.7 in combination with very a high hPPB of 99.97% was discarded. Other liabilities appeared for some compounds when tested for instance for in the human pregnane X receptor (hPXR) assay reflecting induction of cytochrome P450 and playing a role in detoxification. Indeed, compound **97**, **119** and **118** were discarded based on an EC_{50} < 1 µM in this assay. Compounds with non-measurable hPPB, as observed with compound **66** or compound **114** were not favored either. In the following, the detailed pharmacological characterization of our remaining frontrunner **93** is described.

A dose-response of the hydrochloride salt of **93** was performed in male Wistar rats implanted with telemetry transmitters for EEG/EMG recording to evaluate its effect on the sleep-wake cycle (Figure 17). Compound **93** x HCl was formulated in 0.5% methylcellulose and single oral doses of **93** x HCl, equivalent to 0, 10, 30, 100, or 300 mg kg^{-1} of the free base were administered by gavage at the beginning of the nocturnal active phase.

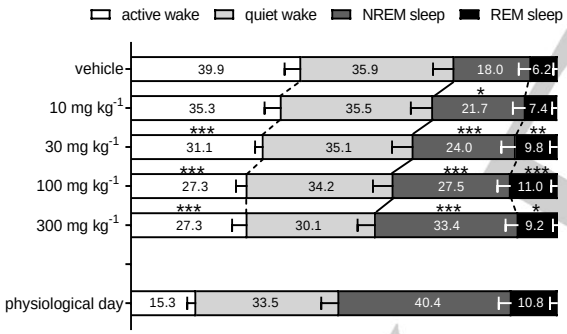

Figure 17. Effect of **93 x HCl** on the time spent in sleep and wake stages (% of total time) in rats. Summary of the 6 h night active period following oral administration of **93 x HCl** formulated in MC0.5%. Doses calculated for free base. Data are expressed as mean ± SEM. One-way ANOVA followed by the post-hoc Dunnett's multiple comparisons test: * p < 0.05, ** p < 0.01, *** p < 0.001 compared to vehicle-treated rats. n = 8/dose group. MC, methycellulose; REM, rapid eye movement; NREM, non-REM.

Over the 6h period following administration, compound **93** x HCl dose-dependently decreased total wake time (one-way analysis of variance (one-way ANOVA; p < 0.0001) by up to 66 min, while increasing REM (up to 17 min) and NREM (up to 55 min) sleep times (one-way ANOVA; p = 0.0008 and p < 0.0001, respectively). The effect of the 10 mg kg^{-1} dose was statistically significant vs vehicle on NREM sleep variables (+13 min, Figure 17); the lowest dose that was statistically significant on all variables was 30 mg kg^{-1}. In addition, the latency to the first persistent episode of NREM sleep (the first NREM sleep episode lasting at least 60 s) and the first persistent episode of REM sleep (the first REM sleep episode lasting at least 30 s) were decreased (one-way ANOVA, p < 0.0001 and p = 0.0065, respectively). Latency to NREM sleep decreased from 61 min for the vehicle-treated rats to 17 min at 10 mg kg^{-1} (p = 0.0006) and down to 11 min at 300 mg kg^{-1} (p < 0.0001) and latency to REM sleep from 63 min to 25 min at 30 mg kg^{-1} (shorter latency observed, p=0.0037). Non-REM and REM sleep increased in physiological proportion, i.e. under **93** x HCl treatment, sleep architecture was conserved, as the relative proportions of non-REM and REM sleep over the total sleep time were not significantly changed (71 to 78% NREM, one-way ANOVA, p = 0.1689).

Compound **93** x HCl was also evaluated in freely moving male Beagle dogs implanted with telemetry transmitters for EEG/EMG recording. Dogs received a single oral dose of 0, 10, 30, or 90 mg of **93** x HCl as an amorphous solid dispersion in gelatin capsules during their day active phase (Figure 18).

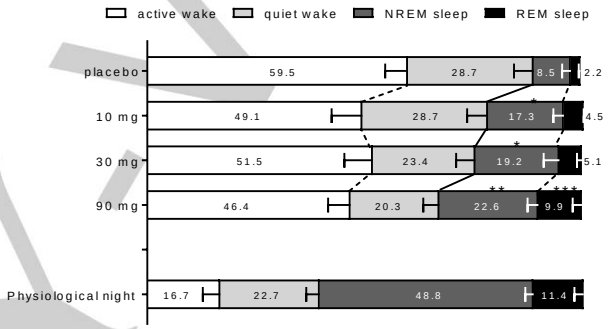

Figure 18. Effect of **93 x HCl** on the time spent in sleep and wake stages (% of total time) in dogs. Summary of the 6 h day active period following oral administration of **93 x HCl** formulated as an amorphous solid dispersion and given in gelatin capsules. Data are expressed as mean ± SEM. One-way ANOVA followed by the post-hoc Dunnett's multiple comparisons test: * p < 0.05, ** p < 0.01, *** p < 0.001 compared to placebo-treated dogs. n = 6-10/dose group. MC, methycellulose; REM, rapid eye movement; NREM, non-REM.

Over the 6 h period following administration, **93** x HCl dose-dependently decreased total wake time (one-way ANOVA; p = 0.0001) by up to 77 min. This decrease in wakefulness was accompanied by increases in both REM (up to 28 min) and NREM (up to 51 min) sleep times (one-way ANOVA; p = 0.0004 and p = 0.002). The effect of the 10 mg/dog dose was statistically significant vs placebo on NREM sleep variables (+ 32 min, Figure 18). In addition, the latency to the first persistent episode of NREM sleep (the first NREM sleep episode lasting at least 60 s) was decreased (one-way ANOVA, p = 0.0448) by 51 to 68 minutes depending on the dose. The decrease only reached statistical significance for the 30 mg dose where the latency decreased from 104 min for the placebo-treated dogs to 35 min (p=0.0451). Similarly to observations in rats, the relative proportions of NREM and REM sleep over the total sleep time were not significantly changed (71 to 81% NREM, one-way ANOVA, p = 0.6058).

Compound **93** was tested in a panel of over 130 enzymes and radioligand binding assays for established central and peripheral pharmacological targets. Compound **93** showed no relevant activity against these targets at the tested concentration of 10 µM. Based on the excellent pharmacology results obtained in rats and dogs, the outcome of the first safety screen and the results of the PB-PKPD modelling work [1], it was decided to develop compound **93** (daridorexant).

Synthesis of **93 (daridorexant)** and analogs (Figure 19):
In the first step, the medicinal chemistry synthesis of compound **89** starts with commercially available N-Boc protected (S)-2-methyl-proline (**A**) which is reacted with 3-methly-4-chloro phenylenediamine (**B**) under standard amide bond forming conditions in dichloromethane using DIPEA as a base and HATU as the coupling reagent. The reaction runs at room temperature over night to give the intermediate **C** as two regioisomers **C1** and **C2** in quantitative yield, which upon cyclization under acidic conditions at 100°C in 1 hour resulted in the same benzimidazole derivative **D** in 49% yield. Boc deprotection by applying standard conditions (HCl in dioxane, 1.6M) at room temperature resulted in the HCl-salt of key intermediate **E**. The preparation of **93 (daridorexant)** required the synthesis of the specific 2-triazolo-5-methoxy-benzoic acid **H**. This was achieved in 76% yield, by reacting the commercially available 2-iodo-5-methoxy-benzoic acid in a copper catalyzed coupling in the presence of cesium carbonate as base, in DMF at 80°C with common 1,2,3-triazole. In the final step, 2-triazolo-5-methoxy-benzoic acid (**H**) is coupled with intermediate **E** in dichloromethane, with DIPEA as the base and HATU as the coupling reagent to yield **93** in 63%. The HCl-salt of **93** was prepared by adding 1 equivalent of 1.6 M HCl in dioxane solution to a slurry of **93** in dioxane followed by evaporation of the solvent and drying of the final material under high vacuum conditions.

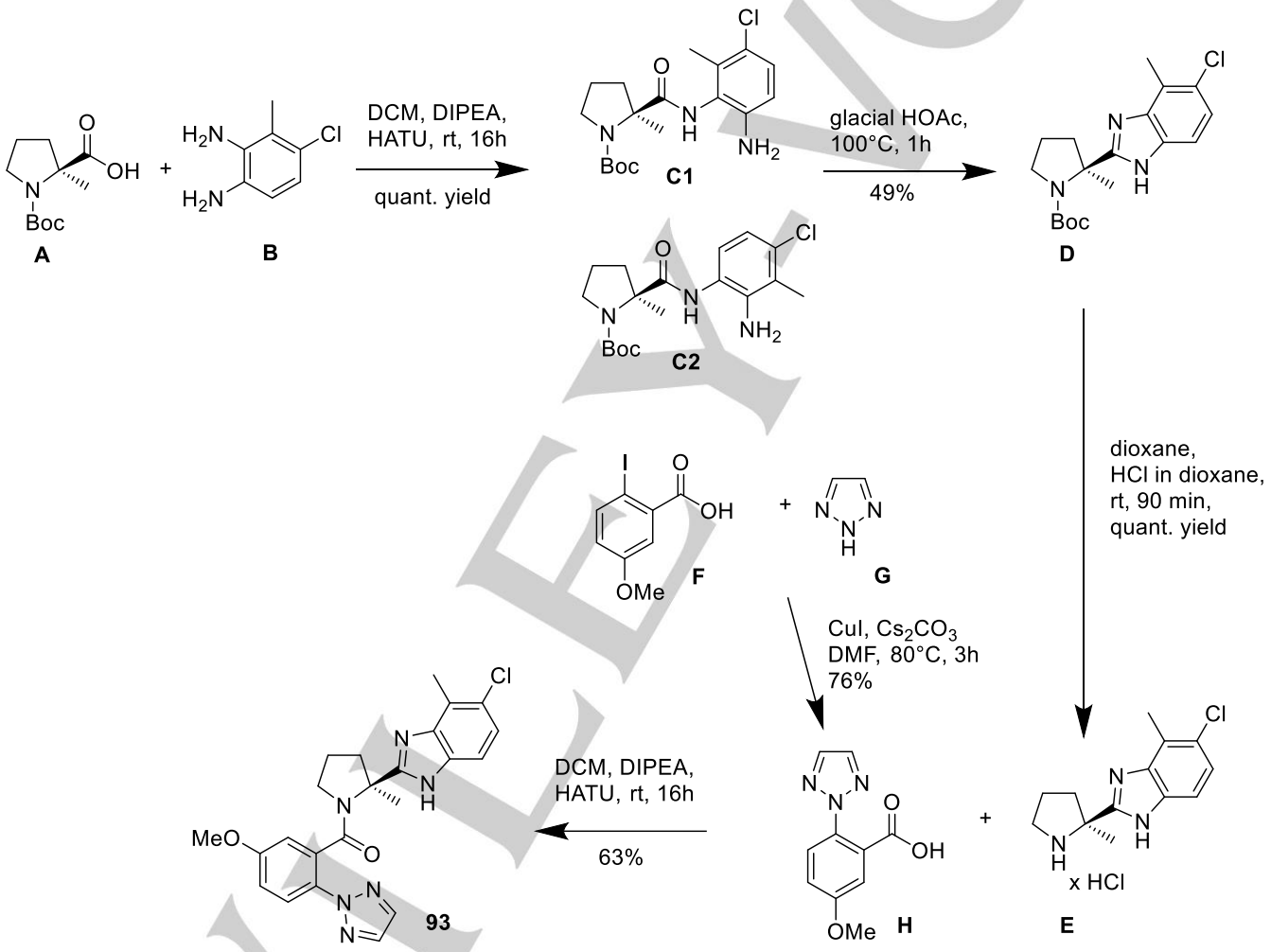

Figure 19. Synthesis of benzimidazole-proline based dual orexin receptor antagonists: Synthesis of 93 (daridorexant) is given as exemplary access to the compounds; all the other compounds described before can be prepared accordingly by adapting the starting materials. Detailed synthetic information for 93 on kg-scale can be found in the supporting information and general procedures in WO 2013/182972.

Conclusion

Taking ACT-462206 (**7**) [38], a proline based dual orexin receptor antagonist, as a starting point for our medicinal chemistry program, we identified a novel series of benzimidazole based orexin receptor antagonists. The major structural changes from **7** to the new series, involved replacing the anilide moiety by a benzimidazole unit and the sulfonamide moiety by triazolyl-substituted benzoyl unit. Extensive medicinal chemistry work, combined with significant characterization efforts in *in vivo* pharmacology of a large number of potent dual orexin receptor antagonists, further *in vitro* characterization for absorption,

distribution, metabolism and excretion (ADME) and safety assessments, resulted in 15 promising DORA compounds. Identification of the best compound out of the 15 frontrunners was finally performed by implementing a PB-PKPD model [1] and assessing additional safety aspects *in vitro*. The efforts culminated in the selection of compound **93**, now called *daridorexant*, for preclinical followed by clinical development. Compound **93** dose-dependently promotes sleep in rats and dogs. The sleep architecture (=relative proportions of REM vs NREM sleep) obtained following administration of **93** is comparable to the architecture of physiological sleep. Compound **93** is in Phase 3 clinical trials for the treatment of insomnia. Top line results of the first pivotal phase 3 study were released on April 20th, 2020. The study demonstrated that daridorexant improved overall sleep and daytime performance of patients with insomnia. Results of the second pivotal study clearly confirmed the results from the first pivotal study.

Experimental Section

Experimental Details are given in the supporting information.

Acknowledgements

Cédric Fischer, Hélène Roellinger, Hélène Massinet, Malvina Louis, Celia Müller-Grandjean, Katalyn Menyhart, Thomas Sasse, Pascal Rebmann, Daniela Krüsi, Ursula Fusco, Marc Candreia, Amandine Boller, Audrey Chardonneau, Daniel Hafner, Christian Barten, Pauline Ligibel, Stephanie Bazire, Jeanine Thanner, Markus Gude, Viktor Ribic, Stephane Delahaye, Isabelle Weber, Fabienne Drouet, Eric Soubieux, Rolf Wuest, Julia Khobzaoui, Aude Weigel, Kristina Kamin, Bruno Capeleto, Pascal Fullhardt, Elise Jacob, Christine Metzger, Sandrine Chopinet, Amandine Fraichard, Michelle Stutz, Maria Ferrand, Patric Dörrwächter, Marco Tschanz, Alice Prud'homme for expert technical support and Francois Jenck, Martin Bolli, Thomas Weller, Martine Clozel and Cedric Vailant for expert discussions..

Keywords: drug design, orexin receptor antagonists, insomnia, G protein-coupled receptors, structure-activity relationship

[1] A. Treiber, R. de Kanter, C. Roch, J. Gatfield, C. Boss, M. von Raumer, B. Schindelholz, C. Muehlan, J. van Gerven, F. Jenck, *J Pharmacol Exp Ther* **2017**, *362*, 489-503.

[2] a) T. Sakurai, A. Amemiya, M. Ishii, I. Matsuzaki, R. M. Chemelli, H. Tanaka, S. C. Williams, J. A. Richardson, G. P. Kozlowski, S. Wilson, J. R. Arch, R. E. Buckingham, A. C. Haynes, S. A. Carr, R. S. Annan, D. E. McNulty, W. S. Liu, J. A. Terrett, N. A. Elshourbagy, D. J. Bergsma, M. Yanagisawa, *Cell* **1998**, *92*, 573-585; b) L. de Lecea, T. S. Kilduff, C. Peyron, X. Gao, P. E. Foye, P. E. Danielson, C. Fukuhara, E. L. Battenberg, V. T. Gautvik, F. S. Bartlett, 2nd, W. N. Frankel, A. N. van den Pol, F. E. Bloom, K. M. Gautvik, J. G. Sutcliffe, *Proc Natl Acad Sci U S A* **1998**, *95*, 322-327.

[3] C. Peyron, D. K. Tighe, A. N. van den Pol, L. de Lecea, H. C. Heller, J. G. Sutcliffe, T. S. Kilduff, *J Neurosci* **1998**, *18*, 9996-10015.

[4] J. Gatfield, C. Brisbare-Roch, F. Jenck, C. Boss, *ChemMedChem* **2010**, *5*, 1197-1214.

[5] T. Matsuki, T. Sakurai, *Results Probl Cell Differ* **2008**, *46*, 27-55.

[6] a) C. Wang, Q. Wang, B. Ji, Y. Pan, C. Xu, B. Cheng, B. Bai, J. Chen, *Front Mol Neurosci* **2018**, *11*, 220; b) J. P. Kukkonen, C. S. Leonard, *Br J Pharmacol* **2014**, *171*, 314-331.

[7] I. Z. Shahid, A. A. Rahman, P. M. Pilowsky, *Vitam Horm* **2012**, *89*, 159-184.

[8] a) J. N. Marcus, C. J. Aschkenasi, C. E. Lee, R. M. Chemelli, C. B. Saper, M. Yanagisawa, J. K. Elmquist, *J Comp Neurol* **2001**, *435*, 6-25; b) P. Trivedi, H. Yu, D. J. MacNeil, L. H. Van der Ploeg, X. M. Guan, *FEBS Lett* **1998**, *438*, 71-75; c) L. de Lecea, *Prog Brain Res* **2012**, *198*, 15-24.

[9] a) A. Eban-Rothschild, L. Appelbaum, L. de Lecea, *Neuropsychopharmacology* **2018**, *43*, 937-952; b) N. Nevarez, L. de Lecea, *F1000Res* **2018**, *7*.

[10] B. Latifi, A. Adamantidis, C. Bassetti, M. H. Schmidt, *Front Neurol* **2018**, *9*, 790.

[11] M. D. Thompson, H. Xhaard, T. Sakurai, I. Rainero, J. P. Kukkonen, *Front Neurosci* **2014**, *8*, 57.

[12] a) G. E. Callander, M. Olorunda, D. Monna, E. Schuepbach, D. Langenegger, C. Betschart, S. Hintermann, D. Behnke, S. Cotesta, M. Fendt, G. Laue, S. Ofner, E. Briard, C. E. Gee, L. H. Jacobson, D. Hoyer, *Front Neurosci* **2013**, *7*, 230; b) D. Hoyer, T. Durst, M. Fendt, L. H. Jacobson, C. Betschart, S. Hintermann, D. Behnke, S. Cotesta, G. Laue, S. Ofner, E. Legangneux, C. E. Gee, *Front Neurosci* **2013**, *7*, 235.

[13] a) T. Nagahara, T. Saitoh, N. Kutsumura, Y. Irukayama-Tomobe, Y. Ogawa, D. Kuroda, H. Gouda, H. Kumagai, H. Fujii, M. Yanagisawa, H. Nagase, *J Med Chem* **2015**, *58*, 7931-7937; b) Y. Irukayama-Tomobe, Y. Ogawa, H. Tominaga, Y. Ishikawa, N. Hosokawa, S. Ambai, Y. Kawabe, S. Uchida, R. Nakajima, T. Saitoh, T. Kanda, K. Vogt, T. Sakurai, H. Nagase, M. Yanagisawa, *Proc Natl Acad Sci U S A* **2017**, *114*, 5731-5736; c) M. Suzuki, H. Yukitake, T. Ishikawa, H. Kimura, **2018**; d) H. Yukitake, T. Ishikawa, A. Suzuki, Y. Shimizu, M. Nakashima, T. Fujimoto, K. Rikimaru, M. Ito, M. Suzuki, H. Kimura, **2018**; e) H. NAGASE, T. SAITOH, M. YANAGISAWA, Y. IRUKAYAMA, *WO2019117148* **2019**; f) Y. KAJITA, S. MIKAMI, Y. MIYANOHANA, T. KOIKE, M. DAINI, N. OYABU, M. OGINO, K. TAKEUCHI, Y. ITO, N. TOKUNAGA, T. SUGIMOTO, T. MIYAZAKI, T. ODA, Y. HOASHI, Y. HATTORI, K. IMAMURA, *WO2019027058* **2019**.

[14] J. Yin, J. C. Mobarec, P. Kolb, D. M. Rosenbaum, *Nature* **2015**, *519*, 247-250.

[15] J. Yin, K. Babaoglu, C. A. Brautigam, L. Clark, Z. Shao, T. H. Scheuermann, C. M. Harrell, A. L. Gotter, A. J. Roecker, C. J. Winrow, J. J. Renger, P. J. Coleman, D. M. Rosenbaum, *Nat Struct Mol Biol* **2016**, *23*, 293-299.

[16] R. Suno, K. T. Kimura, T. Nakane, K. Yamashita, J. Wang, T. Fujiwara, Y. Yamanaka, D. Im, S. Horita, H. Tsujimoto, M. S. Tawaramoto, T. Hirokawa, E. Nango, K. Tono, T. Kameshima, T. Hatsui, Y. Joti, M. Yabashi, K. Shimamoto, M. Yamamoto, D. M. Rosenbaum, S. Iwata, T. Shimamura, T. Kobayashi, *Structure* **2018**, *26*, 7-19 e15.

[17] M. Rappas, A. A. E. Ali, K. A. Bennett, J. D. Brown, S. J. Bucknell, M. Congreve, R. M. Cooke, G. Cseke, C. de Graaf, A. S. Dore, J. C. Errey, A. Jazayeri, F. H. Marshall, J. S. Mason, R. Mould, J. C. Patel, B. G. Tehan, M. Weir, J. A. Christopher, *J Med Chem* **2020**, *63*, 1528-1543.

[18] L. Gershell, *Nat Rev Drug Discov* **2006**, *5*, 15-16.

[19] D. Riemann, K. Spiegelhalder, B. Feige, U. Voderholzer, M. Berger, M. Perlis, C. Nissen, *Sleep Med Rev* **2010**, *14*, 19-31.

[20] S. Schutte-Rodin, L. Broch, D. Buysse, C. Dorsey, M. Sateia, *J Clin Sleep Med* **2008**, *4*, 487-504.

[21] C. M. Morin, C. L. Drake, A. G. Harvey, A. D. Krystal, R. Manber, D. Riemann, K. Spiegelhalder, *Nat Rev Dis Primers* **2015**, *1*, 15026.

[22] M. K. Stoller, *Clin Ther* **1994**, *16*, 873-897; discussion 854.

[23] E. M. Wickwire, F. T. Shaya, S. M. Scharf, *Sleep Med Rev* **2016**, *30*, 72-82.

[24] D. Riemann, M. L. Perlis, *Sleep Med Rev* **2009**, *13*, 205-214.
[25] D. J. Nutt, S. M. Stahl, *J Psychopharmacol* **2010**, *24*, 1601-1612.
[26] J. MacFarlane, C. M. Morin, J. Montplaisir, *Clin Ther* **2014**, *36*, 1676-1701.
[27] L. C. Toner, B. M. Tsambiras, G. Catalano, M. C. Catalano, D. S. Cooper, *Clin Neuropharmacol* **2000**, *23*, 54-58.
[28] a) W. Yang, M. Dollear, S. R. Muthukrishnan, *Arch Phys Med Rehabil* **2005**, *86*, 1265-1266; b) N. Gunja, *J Med Toxicol* **2013**, *9*, 163-171; c) R. H. Farkas, E. F. Unger, R. Temple, *N Engl J Med* **2013**, *369*, 689-691.
[29] a) C. Drahl, *Chemical & Engineering News* **2014**, *92*, 52-55; b) P. Murphy, M. Moline, D. Mayleben, R. Rosenberg, G. Zammit, K. Pinner, S. Dhadda, Q. Hong, L. Giorgi, A. Satlin, *J Clin Sleep Med* **2017**, *13*, 1289-1299; c) Y. Yoshida, Y. Naoe, T. Terauchi, F. Ozaki, T. Doko, A. Takemura, T. Tanaka, K. Sorimachi, C. T. Beuckmann, M. Suzuki, T. Ueno, S. Ozaki, M. Yonaga, *J Med Chem* **2015**, *58*, 4648-4664.
[30] C. Brisbare-Roch, J. Dingemanse, R. Koberstein, P. Hoever, H. Aissaoui, S. Flores, C. Mueller, O. Nayler, J. van Gerven, S. L. de Haas, P. Hess, C. Qiu, S. Buchmann, M. Scherz, T. Weller, W. Fischli, M. Clozel, F. Jenck, *Nat Med* **2007**, *13*, 150-155.
[31] P. Hoever, G. Dorffner, H. Benes, T. Penzel, H. Danker-Hopfe, M. J. Barbanoj, G. Pillar, B. Saletu, O. Polo, D. Kunz, J. Zeitlhofer, S. Berg, M. Partinen, C. L. Bassetti, B. Hogl, I. O. Ebrahim, E. Holsboer-Trachsler, H. Bengtsson, Y. Peker, U. M. Hemmeter, E. Chiossi, G. Hajak, J. Dingemanse, *Clin Pharmacol Ther* **2012**, *91*, 975-985.
[32] a) K. M. Connor, E. Mahoney, S. Jackson, J. Hutzelmann, X. Zhao, N. Jia, E. Snyder, D. Snavely, D. Michelson, T. Roth, W. J. Herring, *Int J Neuropsychopharmacol* **2016**, *19*; b) P. J. Coleman, J. D. Schreier, C. D. Cox, M. J. Breslin, D. B. Whitman, M. J. Bogusky, G. B. McGaughey, R. A. Bednar, W. Lemaire, S. M. Doran, S. V. Fox, S. L. Garson, A. L. Gotter, C. M. Harrell, D. R. Reiss, T. D. Cabalu, D. Cui, T. Prueksaritanont, J. Stevens, P. L. Tannenbaum, R. G. Ball, J. Stellabott, S. D. Young, G. D. Hartman, C. J. Winrow, J. J. Renger, *ChemMedChem* **2012**, *7*, 415-424, 337.
[33] M. A. Letavic, P. Bonaventure, N. I. Carruthers, C. Dugovic, T. Koudriakova, B. Lord, T. W. Lovenberg, K. S. Ly, N. S. Mani, D. Nepomuceno, D. J. Pippel, M. Rizzolio, J. E. Shelton, C. R. Shah, B. T. Shireman, L. K. Young, S. Yun, *J Med Chem* **2015**, *58*, 5620-5636.
[34] T. E. Scammell, E. Arrigoni, J. O. Lipton, *Neuron* **2017**, *93*, 747-765.
[35] A. Palasz, D. Lapray, C. Peyron, E. Rojczyk-Golebiewska, R. Skowronek, G. Markowski, B. Czajkowska, M. Krzystanek, R. Wiaderkiewicz, *Int J Neuropsychopharmacol* **2014**, *17*, 157-168.
[36] a) P. Hoever, S. de Haas, J. Winkler, R. C. Schoemaker, E. Chiossi, J. van Gerven, J. Dingemanse, *Clin Pharmacol Ther* **2010**, *87*, 593-600; b) W. J. Herring, E. Snyder, K. Budd, J. Hutzelmann, D. Snavely, K. Liu, C. Lines, T. Roth, D. Michelson, *Neurology* **2012**, *79*, 2265-2274; c) R. Rosenberg, P. Murphy, G. Zammit, D. Mayleben, D. Kumar, S. Dhadda, G. Filippov, A. LoPresti, M. Moline, *JAMA Netw Open* **2019**, *2*, e1918254.
[37] L. Citrome, *Int J Clin Pract* **2014**, *68*, 1429-1441.
[38] C. Boss, C. Roch-Brisbare, M. A. Steiner, A. Treiber, H. Dietrich, F. Jenck, M. von Raumer, T. Sifferlen, C. Brotschi, B. Heidmann, J. T. Williams, H. Aissaoui, R. Siegrist, J. Gatfield, *ChemMedChem* **2014**, *9*, 2486-2496.
[39] a) C. Brotschi, M. H. Bolli, J. Gatfield, B. Heidmann, F. Jenck, C. Roch, T. Sifferlen, A. Treiber, J. T. Williams, C. Boss, *ChemMedChem* **2020**, *15*, 430-448; b) C. Brotschi, C. Roch, J. Gatfield, A. Treiber, J. T. Williams, T. Sifferlen, B. Heidmann, F. Jenck, M. H. Bolli, C. Boss, *ChemMedChem* **2019**, *14*, 1257-1270.

The quest for the best dual orexin receptor antagonist (daridorexant) for the treatment of insomnia disorders

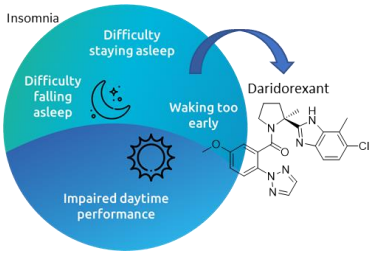

Since its discovery in 1998, the orexin system is of interest to the research community as a potential therapeutic target for the treatment of sleep/wake disorders. We describe our efforts leading to the identification of daridorexant which successfully finished two pivotal phase 3 clinical trials for the treatment of insomnia disorders.